CHALMERS

Modelling of Membrane in a Sodium Sulfate Electrochemical Splitting Cell

Master of Science Thesis in the Master's programme Innovative and Sustainable Chemical Engineering

ADNA H. CARLBERG

Department of Chemistry and Chemical Engineering
Division of Chemical Engineering
CHALMERS UNIVERSITY OF TECHNOLOGY
Gothenburg, Sweden 2015

MASTER OF SCIENCE THESIS

Modelling of Membrane in a Sodium Sulfate Electrochemical Splitting Cell

ADNA H. CARLBERG

Supervisors: Sara Angervall and Mehdi Arjmand
AkzoNobel, Pulp and Performance Chemicals

Examiner: Prof. Anders Rasmuson
Chalmers, Chemical Engineering Design

Department of Chemistry and Chemical Engineering
Division of Chemical Engineering
CHALMERS UNIVERSITY OF TECHNOLOGY
Gothenburg, Sweden 2015

Modelling of Membrane in a Sodium Sulfate Electrochemical Splitting Cell

ADNA H. CARLBERG

Master of Science Thesis
Department of Chemistry and Chemical Engineering
Division of Chemical Engineering
Chalmers University of Technology
SE-412 96 Gothenburg
Sweden
Telephone: + 46 (0)31-772 1000

Gothenburg, Sweden 2015

Modelling of Membrane in a Sodium Sulfate Electrochemical Splitting Cell

ADNA H. CARLBERG

Department of Chemistry and Chemical Engineering
Division of Chemical Engineering
Chalmers University of Technology

Abstract

The master's thesis aims at obtaining a deeper understanding of the transport phenomena in a sodium sulfate electrochemical splitting cell. This is done by modelling the ion transport through a cation exchange membrane Nafion, both with and without adjacent boundary layers.

The resulting model is derived from the Nernst-Planck equation and after some simplification the model includes the terms diffusion and migration. An analytical solution of the model equation is compared with two numerical solutions by looking at the concentration profiles for the moving species (sodium ions, hydrogen ions and hydroxyl ions). Also the fluxes of the ions, pH, water transport and electric potential through the membrane are investigated by profile plots. All profiles show expected results, except the concentration profile in the anolyte film when boundary layers are added.

The main modelling parameters are found to be the bulk concentrations, for the boundary conditions, and diffusivities for the ions. The potential drop, permittivity and thickness of film layers are found to be important. A major limitation of the modelling procedure in the thesis is though lack of data, especially parameters describing the membranes is difficult to obtain estimates for. Apart from the conceptual and mathematical modelling, verification of the mathematical solution by comparison with formerly obtained results in the literature and finally experimental validation of the model remain.

Keywords: electrochemical splitting, sodium sulfate, Nafion membrane, ion transport, Nernst-Planck, modelling, MATLAB.

Acknowledgements

I would like to acknowledge my supervisors Sara Angervall and Mehdi Arjmand for all their help, commitment and advice. They have been a great support throughout the thesis work. I would also like to thank the examiner Anders Rasmuson for guidance and providing valuable input when discussing different ideas.

I would like to express my gratitude to Kalle Pelin, the department manager of Process RD&I, for giving me the opportunity to conduct the thesis work at AkzoNobel in Bohus and for giving valuable direction and feedback. Also many thanks to all the people at Process RD&I for a warm welcome to the department and showing interest in the thesis work.

Adna H. Carlberg, Gothenburg, June 2015

Contents

Notations xi
1 Introduction 1
1.1 Background 1
1.2 Purpose 2
1.3 Research questions 2
1.4 Delimitations 2
1.5 Thesis outline 3
2 Theory 5
2.1 Electrochemical splitting 5
2.1.1 Nafion membrane structure 6
2.1.2 Membrane state 6
2.2 Chemistry in the cell 7
2.3 Transport phenomena in the membrane 8
2.3.1 Mass transfer of ions 8
2.3.2 Mass transfer of solvent/water 10
2.3.3 Heat transfer 11
2.3.4 Momentum transfer 11
2.4 Boundary layers near membrane surface 12
2.5 Electrochemical equations 12
3 Methodology 15
3.1 Literature study 15
3.2 Modelling procedure 15
3.3 Solution methods 17
3.3.1 Finite difference method 18
3.3.2 Boundary and initial conditions 18
3.4 Experimental setup 18
3.5 Modelling parameters 19
3.5.1 Modelling boundary and initial conditions 21
3.6 Modelling settings 22
4 Results and Discussion 23
4.1 Model simplification 23
4.1.1 Dimensions and independent variables 23
4.1.2 Convection vs diffusion term 24
4.1.3 Migration vs diffusion term 24
4.1.4 Migration vs convection term 25
4.1.5 Final simplified model 26
4.2 Solution structure of model equations 26
4.2.1 Analytical solution of BVP 26
4.2.2 Numerical solution of BVP 27

4.2.3 Numerical solution of PDE ... 28
4.3 Concentration and flux profiles ... 29
4.4 pH profile ... 31
4.5 Electric potential profile ... 31
4.6 Water transport ... 32
4.7 Boundary layers ... 33
4.7.1 Concentration profiles ... 33
4.7.2 pH profile ... 34
4.7.3 Electric potential profile ... 35
4.8 Influence of impurities ... 36
4.9 Model limitations ... 36
4.9.1 Model simplifications ... 37
4.9.2 Influence of bi-layer membrane ... 37
4.9.3 Electric potential and electro-neutrality ... 37
4.9.4 Boundary layers close to membrane ... 38
4.9.5 Flow phase of electrolytes ... 38
4.9.6 Experimental validation ... 39
5 Conclusions ... 41
6 Future Work ... 43
References ... 45
A Modified Nernst-Planck Equation ... I
B Calculations of Parameters for Modelling ... III
B.1 Calculation of potential drop in boundary layers ... III
B.2 Calculation of permittivity for electrolytes ... III
B.3 Calculation of velocity through the membrane ... IV
B.4 Calculation of free acidity in electrolytes ... IV
B.5 Calculation of sulfonate concentration in membrane ... V
C Peclet Number ... VII
D MATLAB-code for Modelling with BVP ... IX
D.1 BVP script file ... IX
D.2 Function files ... XI
E MATLAB-code for Modelling with PDE ... XIII
E.1 PDE script file ... XIII
E.2 Function files ... XVI
F Surface Plots for Concentration Profiles ... XIX

Notations

Variables used in equations in the thesis are presented here with symbol, description and unit:

A	Unit area	[m^2]
α	Anolyte volume variation per charge	[dm^3/mol]
α_i^θ	Expression of secondary reference state	[dm^3/mol]
CE	Current efficiency	[-]
c_i	Concentration of species i	[mol/dm^3]
D_i	Diffusion coefficient of species i	[m^2/s]
δ_L	Laminar boundary layer	[m]
δ_T	Turbulent boundary layer	[m]
EW	Equivalent weight	[g/mol]
ε	Permittivity or dielectric constant	[F/m]
ε_r	Relative permittivity	[-]
ε_0	Vacuum permittivity	[F/m]
F	Faraday's constant	[A·s/mol]
f_i	Molar activity coefficient of species i	[-]
h	Mesh interval	[m]
I	Electric current	[A]
i	Current density	[A/m^2]
k	Permeability	[m^2]
k_h	Thermal conductivity	[J/K·s]
κ	Electronic conductivity	[S/m]
L	Thickness of membrane	[m]
M_i	Molar mass of species i	[g/mol]
μ	Dynamic viscosity	[Pa·s]
μ_i	Electrochemical potential of species i	[J/mol]
N_i	Flux of species i	[mol/m^2·s]
n	Number of electrons transferred	[-]
O	Error	[mol/ m^2]
P	Pressure	[Pa]
P_j^i	Perm-selectivity of ion i relative j	[-]
Pe	Peclet number	[-]

Φ	Electric potential	[V]
ϕ	Porosity	[-]
q	Porous flow	[$m^3/m^2 \cdot s$]
q_h	Heat flow	[$J/m^2 \cdot s$]
R	Ideal gas constant	[J/mol·K]
R_i	Production rate of species i	[$mol/dm^3 \cdot s$]
Re_x	Local Reynolds number	[-]
ρ	Density	[g/dm^3]
ρ_a	Density of anolyte	[g/dm^3]
ρ_m	Density of membrane	[g/dm^3]
s	Active surface area	[m^2]
T	Temperature	[K]
$T_{m,i}$	Transport number of species i (based on one ion)	[-]
t	Time	[s]
$t_{m,i}$	Transport number of species i (based on one Faraday)	[-]
u_i	Mobility of species i	[$m^2 \cdot mol/J \cdot s$]
V	Volume	[dm^3]
V_a	Volume of anolyte	[dm^3]
V_c	Volume of catholyte	[dm^3]
V_i	Partial molar volume	[m^3/mol]
v	Velocity of fluid	[m/s]
W	Specific flow rate of water	[$g/m^2 \cdot s$]
x	Distance	[m]
z_i	Valence/charge number of species i	[-]

1 Introduction

The process industry has for the last two centuries found impressive use of earth's resources. It has improved the quality of life for millions of people, but sometimes at the cost of environmental pollutions. Taking care of earth's resources in an efficient and sustainable way, both environmentally and economically, has been the motivation for many companies to improve the use of raw material and energy. Chemical waste recovery is one important approach to achieve a sustainable and environmental friendly process among industries. In the pulp and paper industry for instance, the Kraft pulp mills today have often very efficient chemical recovery systems and low losses of pulping chemicals [1]. But with increasing demands on more extensive closure of systems, there exists a continuous need for improving the use of chemicals.

1.1 Background

AkzoNobel is an international company that is a supplier of decorative paints, performance coatings and a large number of specialty chemicals. One of these specialty chemicals is sodium chlorate ($NaClO_3$) which is used to produce chlorine dioxide (ClO_2). Chlorine dioxide is a powerful oxidizing agent and it is used as a bleaching chemical in the pulp industry, mostly in the Kraft process [1]. Manufacturing processes of chlorine dioxide [2] result in a by-product, which is sodium sulfate (Na_2SO_4) and often referred to as salt cake [1, 3]. It may be beneficial to convert this by-product into more valuable feedstock such as sodium hydroxide ($NaOH$) and sulfuric acid (H_2SO_4), see Figure 1. In order to do so, one approach is to split the sodium sulfate using an electrochemical cell including an ion exchange membrane to promote the selectivity [1, 3, 4, 5, 6].

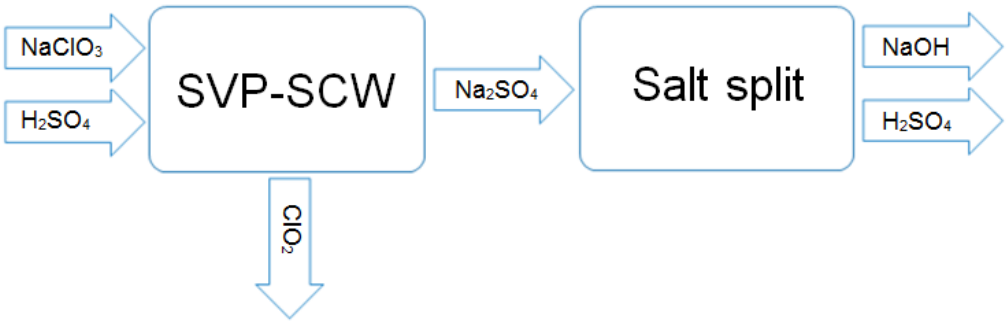

Figure 1: Overview of chemicals involved in the chlorine dioxide production in a single vessel process (SVP) with salt cake wash (SCW) [2] and in a salt split unit.

Sustainability is an important consideration for AkzoNobel in all stages of the value chain. Even if the main objective of the salt split process is to upgrade the value of the by-product salt, there are several interests for developing alternative use of the sulfate by-product [1, 3]. In the future there could be limited permissions for emission of the by-product and disposal can be very costly, especially if the sodium sulfate

includes impurities [4]. For the splitting of sodium sulfate, substantial electric energy is required which may be available on the mill and thus constitute an advantage from a sustainability perspective as this energy is bio-based [3]. The conversion of sodium sulfate can also give substantial benefits for the pulp mills if cost for raw material increases [1].

1.2 Purpose

The purpose of the master's thesis is to obtain a deeper understanding of the electrochemical processes in a cell for splitting sodium sulfate. This will mainly be done by modelling a cation exchange membrane, primarily Nafion 324, to investigate some of the transport phenomena in the cell. It is aimed that the gained knowledge can be later used for improving the process and the obtained model could be useful for upscaling to production scale or when using different types of membranes.

1.3 Research questions

The focus of this thesis is to investigate what is happening in the cell by studying the transport phenomena in the membrane. For this purpose, the following research questions are considered:

- What types of model equations are useful to describe the transport of molecules through the membrane?
- What parameters are important when deriving a membrane model?
- How are cations (sodium ions, Na^+, and hydrogen ions, H^+) transported through the membrane?
- How large is the water transport through the membrane based on different conditions in the cell?
- How does the proton profile vary from the acidic side to caustic side?
- How does the ionic concentration profile look like around the membrane?
- How do other ions (e.g. calcium ions, Ca^{2+}, or potassium ions, K^+) due to impurities, affect the transportation through the membrane?

1.4 Delimitations

The anolyte and catholyte compartments are considered separated and interconnected by the transport of species through the membrane. Initially only the transport across the membrane is considered, but later also boundary layers are included. In the thesis, parameters for the Nafion 324 membrane are used as far as possible. However, the derived model should be useful for any type of membrane as long as the diffusivities of the molecules and the thickness of the membrane is known.

In a large scale salt split cell the composition of the electrolyte, void fractions etc. at the inlet and at the outlet of the cell are different. Hence the conditions lead to different results for the transport phenomena. However as the dimensions of the electrochemical cell this work can be validated against are small, the modelling only accounts for the transport in one dimension (perpendicular to the membrane) and the conditions over the cell passage are averaged to those of a half passage in this thesis.

The temperature along the cell passage and between the two compartments in a small scale salt split cell is very similar. Heat transfer over the membrane is thus neglected in the absence of temperature gradient i.e. the driving force is zero or very small.

In the thesis, the modelling of the fluid in the cell is limited to single phase modelling. Thus the two-phase flow nature of the process due to the presence of gas (hydrogen, H_2, and oxygen, O_2) produced at the electrodes is neglected.

1.5 Thesis outline

The thesis is composed of 6 chapters, a reference list and 6 appendices.

Chapter 1 – Introduction contains the background and objective for the master thesis is presented, as well as delimitations and research questions for the purpose.

The knowledge obtained from the literature study is gathered in Chapter 2 – Theory, describing electrochemical splitting with a cation exchange membrane and the chemistry in the cell. The transport phenomena through the membrane are also described with relevant equations for the modelling of ion transport.

Chapter 3 – Methodology describes the different steps in the modelling procedure, the experimental setup and the parameter values used in the modelling.

The model structure, concentration profiles and flux profiles are presented in Chapter 4 – Results and Discussion, together with the analysis of the results and model limitations.

Some the final remarks from the thesis are summarized in Chapter 5 – Conclusions.

Chapter 6 – Future Work includes some recommendations for proceeding modelling.

2 Theory

In this section the theoretical framework for the electrochemical salt split cell is presented, i.e. electrolysis, membrane structure, chemistry in the cell and governing equations for the transport phenomena through the membrane are described.

2.1 Electrochemical splitting

Salt splitting can be achieved by electrolysis. In electrolysis, chemical compounds are decomposed by using a direct electric current. To perform salt splitting by electrolysis a cell with two electrodes, an anode and a cathode, is needed as shown in Figure 2 [7]. The anode is the positive electrode which attracts anions and it is where oxidation occurs. The cathode is the negative electrode which attracts cations and it is where reduction occurs. The cell is filled with electrolyte, which is a solution of water or other solvents in which ions are dissolved [7]. The electrolyte blocks the movement of electrons and by applying a decomposition potential, i.e. the voltage needed for the electrolysis to occur, the motion of the ions towards the charged electrode is made possible [7, 8]. The current density can be measured as the electric current per unit cross section area [8].

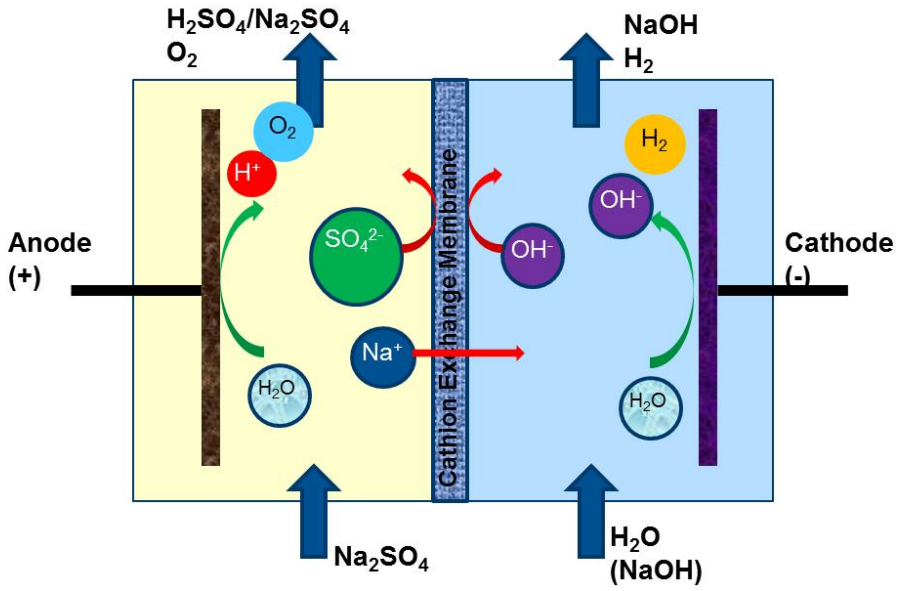

Figure 2: A two compartment salt split cell with cation exchange membrane (CEM) [1] (with permission of copywrite owner).

Cation exchange membrane (CEM) is used to separate the electrolyte into an anolyte and a catholyte compartment. Due to the composition of the membrane it allows the motion of only cations through the membrane governed by an electrostatic field [1]. Also, electro-osmosis which is the motion of solvent (water) through the membrane due to the applied electrical field can occur [8], which is further described in Section 2.3.2.

2.1.1 Nafion membrane structure

The ion exchange membrane used in the electrochemical cell is made up of a polymer composite matrix called Nafion® N324. The microstructure of the polymer consists of a strong hydrophobic fluorocarbon/polytetrafluoroethylene backbone with sidechains which end with a hydrophilic sulfonic acid [9, 10, 11], see Figure 3. The Nafion membrane allows cation transport through the polymer by exchange with the proton from the sulfonic acid [10], and works as a barrier towards anions by repulsion with the negatively charged fixed sulfonate groups [8]. The hydrated sulfonic acids can also form inclusions with water which sustain the ion conduction. When Nafion is used as a separator in an electrochemical cell, the electron flux on the electrode surface is balanced by the ion flux through the membrane [10].

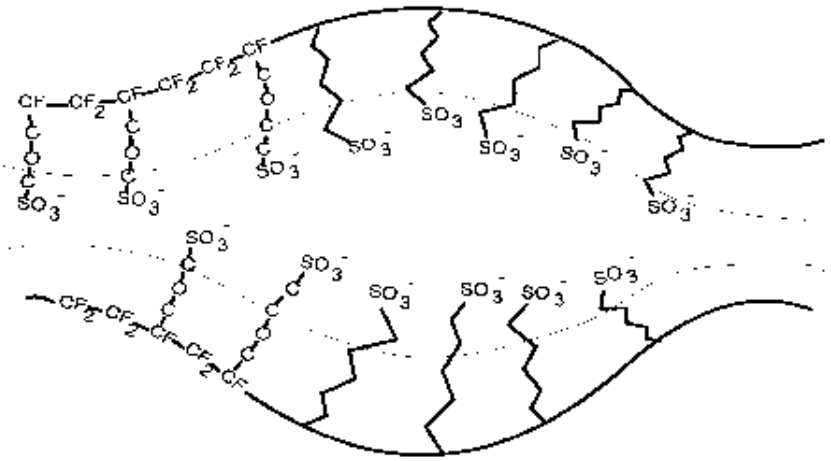

Figure 3: The microstructure of the Nafion membrane, adapted from [12] (with permission of copywrite owner).

The N324 is a bi-layer membrane which is reinforced and consists of two sulfonate layers of different equivalent weight (EW) with different concentration of fixed negative charge [13]. Studies have shown that the membrane consists of a channel network with very small pore channels in the size range of nanometers [11]. The Nafion membrane 324 is one of the best performing cation exchange membranes based on current efficiency measurements [13]. It has also been shown that the hydraulic permeability across Nafion membranes increases with increasing temperature and decreasing equivalent weight [11].

2.1.2 Membrane state

There are two models defined for the state of a membrane, the acid membrane state and the alkaline membrane state [4], see Figure 4.

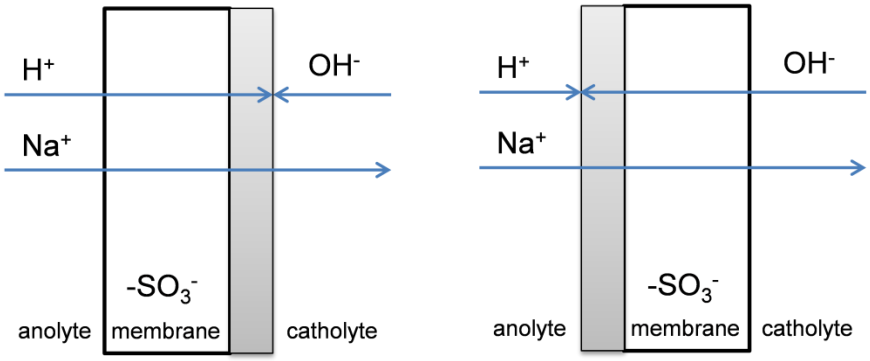

Figure 4: Model of the acid membrane state (to the left) and the alkaline membrane state (to the right) of a cation exchange membrane.

In the acid membrane state, the catholyte concentration has no influence on the current efficiency because hydroxyl ions have already been neutralized in the acid boundary layer [4, 14]. Hydrogen ions pass the membrane when the acid concentration is high and the sodium hydroxide concentration is low [5].

For the alkaline membrane state, the acid concentration in the anolyte has no influence on the current efficiency because hydrogen ions have already been neutralized in the alkaline boundary layer [4, 14]. Hydroxyl ions pass the membrane when the acid concentration is low and the sodium hydroxide concentration is high [5].

2.2 Chemistry in the cell

The electrochemical splitting of sodium sulfate results in formation of sulfuric acid (H_2SO_4), and sodium hydroxide ($NaOH$) [1]. Sodium sulfate is fed to the cell with the anolyte and water is used for the catholyte, see Figure 2.

The overall reaction takes place in two steps; splitting of water into ions (H^+ and OH^-) at the electrodes and separation of sodium ions (Na^+) and sulfate ions (SO_4^-) by transportation over the membrane [4]. The following reactions occur in the cell [1]:

Anode reaction: $2\ H_2O \rightarrow 4\ H^+ + O_2 + 4e^-$ (1)

Cathode reaction: $4\ H_2O + 4e^- \rightarrow 4\ OH^- + 2\ H_2$ (2)

Total reaction: $6\ H_2O \rightarrow 4\ OH^- + 2\ H_2 + 4\ H^+ + O_2$ (3)

Overall reaction: $2\ Na_2SO_4 + 6\ H_2O \rightarrow 4\ NaOH + 2\ H_2SO_4 + 2\ H_2 + O_2$ (4)

Thus, in the anode compartment water is oxidized into hydrogen ions and oxygen and in the cathode compartment water is reduced to hydroxyl ions and hydrogen. The overall reaction is obtained by including sodium sulfate to the total reaction and thus generating the caustic, sodium hydroxide, and sulfuric acid as a result.

During operation several other reactions might occur due to impurities in the sodium sulfate as a rest product from the chlorine dioxide production [1]. Other phenomena that

also may influence the reactions in the cell are for example damages of the membrane, corrosion of the electrodes or electrical issues [15].

2.3 Transport phenomena in the membrane

Sodium ions and hydrogen ions migrate through the cation exchange membrane towards the cathode due to an induced driving force by the electric field between the electrodes [1, 4, 16]. The hydrogen ion transfer decreases the current efficiency, which varies either with the ratio of sulfuric acid to total sulfate concentration in the anolyte or with sodium hydroxide concentration depending on the state of the membrane (acidic or alkaline) [5]. Migration of hydroxide ions is highly undesired [1].

Water transport occurs through the membrane due to electro-osmosis, from the anolyte to catholyte [5]. Also it seems that sodium ions migrate through the membrane with four water molecules per ion and hydrogen ions migrate with three (or less) water molecules per ion [5], due to coordination chemistry. It has been shown that water flux increases in the current flow direction due to the electro-osmotic drag [16]. Due to a pressure difference in the cell, water can also be transported from one cell compartment to the other [11].

When studying the transport through the cation exchange membrane in the electrochemical cell, one can consider the so-called two-film theory and think of resistance in series to produce concentration profiles [17]. In this thesis the film resistance is initially neglected due to assumed turbulent bulk flow, so the resistance of the transport of ions lies in the membrane itself. Thus only equations describing transport across the membrane is formulated. But even if the flow of electrolyte is considered turbulent there might be boundary layer effects (film resistance) adjacent to the surface of the membrane and for this case a boundary layer model is formulated in a second step.

To obtain a model for the ion transport through the membrane, some governing equations are needed. The membrane modelling can be done on a molecular, microscopic, mesoscopic and macroscopic description level [18]. If the transport process acts as a continuum, i.e. microscopic level, the balance equations for momentum, mass and energy are formulated as differential phenomenological equations and the detailed molecular interactions can be ignored [18].

2.3.1 Mass transfer of ions

Nernst-Planck equation describes the molar flux of ions throught the membrane [7, 8, 13]. The equation is only valid for dilute solutions and the transport of the molecules is a combination of diffusion, migration and convection [7, 8, 19]:

$$N_i = -D_i \nabla c_i - z_i u_i F c_i \nabla \Phi + v c_i \quad (5)$$

The diffusion term comes from Fick's law and describes the flow of the species due to a concentration gradient [19]. The migration is due to the gradient of electric potential and

the convective part is induced by the bulk motion contribution [17]. Since the Nernst-Planck equation is restricted to dilute solutions, it means that solute-solute interactions are neglected and only solute-solvent interactions are considered [20]. To account for these solute-solute interactions, mixture rules with individual diffusion coefficients can be used [20]. Also modifications of the Nernst-Planck equation can be done for moderately dilute solutions [7]. Then a concentration dependent factor for the activity coefficient in the chemical potential is introduced, see Appendix A.

The mass conservation law is valid for each ionic species in the solution, where the accumulation of specie i in a control volume is equal to the divergence of the flux density, $-\nabla N_i$, and source term R_i [7]:

$$\frac{\partial c_i}{\partial t} = -\nabla N_i + R_i \tag{6}$$

Combining the conservation law and Nernst-Planck equation, and assuming no reaction and thus no source term, gives the complete Nernst-Planck equation:

$$\frac{\partial c_i}{\partial t} = -\nabla(-D_i \nabla c_i - z_i u_i F c_i \nabla \Phi + v c_i) \tag{7}$$

Inserting Nernst-Einstein relation, equation (8) for the mobility [7] gives:

$$u_i = \frac{D_i}{RT} \tag{8}$$

$$\frac{\partial c_i}{\partial t} = D_i \nabla^2 c_i + \frac{z_i F D_i}{RT} \nabla c_i \nabla \Phi - v \nabla c_i \tag{9}$$

For positively charged and negatively charged ions, the complete Nernst-Planck equations are respectively:

$$\frac{\partial c_i^+}{\partial t} = D_i \nabla^2 c_i^+ + \frac{z_i F D_i}{RT} \nabla c_i^+ \nabla \Phi - v \nabla c_i^+ \tag{10}$$

$$\frac{\partial c_i^-}{\partial t} = D_i \nabla^2 c_i^- + \frac{z_i F D_i}{RT} \nabla c_i^- \nabla \Phi - v \nabla c_i^- \tag{11}$$

Conservation of volume of the solution is expressed by assuming incompressible solution [20]:

$$\sum_i \mathrm{V_i c_i} = 1 \tag{12}$$

The mobility of the cations is determined by their size and electrical properties, as well as the medium structure [8]. Assuming no current loss at the inlet and outlet pipes, the current efficiency is equal to the sodium transport number, $\mathrm{t_{m,Na^+}}$ [5]. The dimensionless transport number for sodium is defined as the sodium flux through the membrane during a certain time divided by the number of moles of charge transferred in the cell [5]:

$$t_{m,Na^+} = \frac{(V_c[Na^+]_c)_{t+\Delta t} - (V_c[Na^+]_c)_t}{s\Delta t i/F} = \frac{(V_a[Na^+]_a)_{t+\Delta t} - (V_a[Na^+]_a)_t}{s\Delta t i/F} \tag{13}$$

The yield can be defined as the membrane perm-selectivity. Perm-selective coefficient of sodium ion relative hydrogen ion, $P_{H^+}^{Na^+}$ [5]:

$$P_{H^+}^{Na^+} = \frac{t_{m,Na^+}[H^+]}{t_{m,H^+}[Na^+]} \tag{14}$$

Relations describing the ion transport and thus the current transport, in the acidic and alkaline membrane state [5] are respectively:

$$t_{m,Na^+} + t_{m,H^+} = 1 \tag{15}$$

$$t_{m,Na^+} + t_{m,OH^-} = 1 \tag{16}$$

2.3.2 Mass transfer of solvent/water

The solvent, i.e. water in this case, can be transported through the ion exchange membrane in three ways [8]; coupling with the electric current passing the membrane due to the electrical potential gradient (electro-osmosis), transport due to flux of ions with a hydration shell, and transport due to a chemical potential gradient, i.e. concentration gradient, of the solvent (osmotic flux). Depending on the current density, concentration gradient, and perm-selectivity of the ion exchange membrane the three terms can be of different importance [8]. If the membrane is high perm-selective and the difference of salt concentration in the two compartments is moderate, the solvent flux will be dominated by electro-osmosis and flux by hydrated ions [8]. This means that the osmotic solvent flux can be neglected. Also due to the hydrophobic perfluorinated Nafion membrane, the water transport occurs mostly by hydrated ions which are migrating through the membrane as a result of an electrical potential gradient [5, 8].

The water flux, N_{H_2O}, due to electro-osmosis and thus transportation of hydrated ions can be approximated by a solvent transport number multiplied by the flux of ions [8]:

$$N_{H_2O} = T_{m,H_2O} \sum_i N_i \tag{17}$$

The water transport number, T_{m,H_2O}, is defined as the number of water molecules transported through the membrane by one ion. The electro-osmotic water transport number can also be defined as the number of water molecules transported when one Faraday passes through the system [5, 8]:

$$t_{m,H_2O} = \frac{N_{H_2O}}{i/F} = \frac{W/M_{H_2O}}{i/F} \tag{18}$$

The specific flow rate of water through the membrane, W, can be derived by mass balance over the anode compartment and assuming constant density of anolyte [5]:

$$W = \frac{i}{F}\left(\alpha\rho_a - \left(t_{m,Na^+}M_{Na^+} + \left(1 - t_{m,Na^+}\right)M_{H^+}\right) - \frac{M_{O_2}}{4}\right) \tag{19}$$

If the membrane is in acidic state, see Figure 5, the transport number of water represents the number of water molecules (in this case around three) transported by one mole of cations (Na^+ and H^+) [5]. Different cations can have different electro-osmotic transport

numbers of water; ions with rather large hydration shells can have water transport number up to eight, while for example hydrogen ions have a very low number of less than three [8].

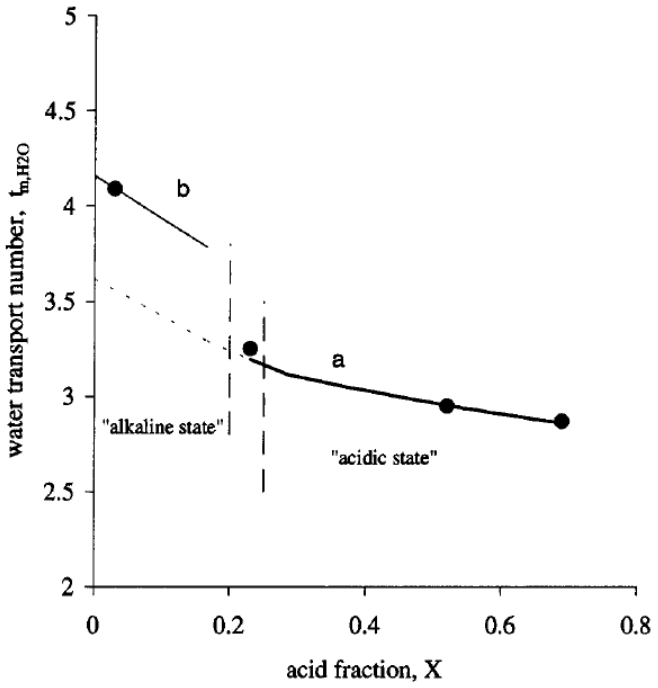

Figure 5: Water transport number against sulfuric acid to sulfate concentration ratio (a) and water to sodium molar ratio during transfer through the membrane in the alkaline membrane state (b) [5] (with permission of Springer Science+Business Media).

An increase of salt concentration can lead to a decrease of water transport number [8]. This is because the perm-selectivity of the membrane decreases with higher salt concentration and leads to substantial transport of co-ion in the opposite direction.

2.3.3 Heat transfer

To account for the heat transfer over the membrane an energy balance is derived with the temperature gradient as driving force. The conduction, which is described through Fourier equation, can be expressed by [17]:

$$q_h = -k_h \frac{dT}{dx} \tag{20}$$

In this thesis, the temperature gradient between the two compartments in the cell is very small and a temperature difference of some few degrees will have very limited effect. Also the viscosity and diffusivity coefficient in the membrane is weakly dependent of the temperature.

2.3.4 Momentum transfer

Darcy's equation is an expression of conservation of momentum and it is used to describe the flow through porous material [18]:

$$q = -\frac{k}{\mu}\frac{\partial P}{\partial x} \quad (21)$$

The Nafion membrane is seen as a porous polymer material and Darcy's equation is used to determine the velocity through the membrane, which can be calculated by dividing the flow with the porosity:

$$v = \frac{q}{\phi} \quad (22)$$

2.4 Boundary layers near membrane surface

Boundary layers (film resistance) at each side of the membrane can be considered, to investigate how the ion concentration profiles look around the membrane. Classification of the boundary layer can be determined by the local Reynolds number [17]:

$$Re_x = \frac{\rho v x}{\mu} \quad (23)$$

If $Re_x < 2 \cdot 10^5$ → Laminar boundary layer

If $2 \cdot 10^5 < Re_x < 3 \cdot 10^6$ → Either laminar or turbulent boundary layer

If $Re_x > 3 \cdot 10^6$ → Turbulent boundary layer

For laminar boundary layers, the Blasius equation can be used over a flat plate [17]:

$$\delta_L \approx \frac{4.91 \cdot x}{\sqrt{Re_x}} \quad (24)$$

For a turbulent boundary layer the thickness is [17]:

$$\delta_T \approx \frac{0.382 \cdot x}{\sqrt{Re_x}} \quad (25)$$

2.5 Electrochemical equations

Current efficiency (Faradaic efficiency), CE, is the ratio of moles of produced product from an electrolyte to the maximum theoretical production, i.e. the equivalent number of moles of electrons passed [13, 21]:

$$CE = \frac{nFV}{It}\Delta c_i \quad (26)$$

It has been found that the overall current efficiency of the salt split cell is determined by the performance of the reactions at the electrodes and by the selectivity of the membrane [1]. Also back-migration of hydroxyl ions or undesired reactions in the cell due to impurities influences the current efficiency negatively. To keep high selectivity and prevent migration of hydrogen ions over the membrane, the conversion of sodium sulfate should be kept at about 50-60% [1] in a two compartment cell.

The current through a membrane is assumed to only be carried by ions and the current density, i (index j is also often used) can be expressed by [7, 8]:

$$i = \frac{I}{A} = F \sum_i z_i N_i \quad (27)$$

The current density is also described by Ohm's law [7]:

$$i = -\kappa \nabla \Phi \tag{28}$$

When solving the Nernst-Planck equations, the potential distribution is needed. The potential distribution can be described with the Poisson equation, where the potential distribution can be calculated from the ionic concentrations [10, 22]:

$$\varepsilon \nabla^2 \Phi + F \sum_i z_i c_i = 0 \tag{29}$$

Where the permittivity, ε, is the product of relative permittivity for the medium and the vacuum permittivity:

$$\varepsilon = \varepsilon_r \varepsilon_0 \tag{30}$$

The Poisson equation together with the Nernst-Planck equations forms the Poisson-Nernst-Planck (PNP) model which is an effective coupling of the transport of individual ions [22]. Poisson equation is used when there is large electric fields and considerable separation of charges [7]. This requires very large electric forces or very small length scales [22].

It is common to assume electro-neutrality when deriving the potential distribution [7, 8, 20]. This occurs when the net charge either locally or globally is zero, meaning that the negative charge is balanced out by the equally large positive charge [8, 10]. This electro-neutrality is expressed by [7]:

$$\sum_i z_i c_i = 0 \tag{31}$$

Mathematically, the electro-neutrality together with the conservation of charge statement for fairly constant concentrations and constant conductivity can be expressed by Laplace's condition on the potential [7, 10]:

$$\nabla^2 \Phi = 0 \tag{32}$$

On a macroscopic scale, electro-neutrality is required for any electrolyte solution or for a solid phase such as the ion-exchange membrane [8]. The fixed negative charges in the Nafion membrane are balanced out by cations, meaning that the counter-ions will be attracted into the membrane and co-ions repelled [8].

3 Methodology

For the master's thesis a literature study and a pre-study of the experimental setup was conducted in order to perform the modelling part and to achieve the aim of the project. Evaluation of the results and report writing are also important parts of the working process.

3.1 Literature study

The literature study was performed throughout the project to increase the knowledge of the area of interest and to get an understanding of the electrochemical phenomena present in the salt split cell. Also a pre-study of the laboratory setup was done in the beginning of the project in order to understand the electrochemical cell and to investigate what data is available for the modelling phase.

Searches of literature (reports, journal articles, books, etc.) were done in databases available from AkzoNobel and through Chalmers Library. Also searches of internal publications and reports in AkzoNobel were carried out. The main focuses of the literature study were to find model equations of transport phenomena in membranes, to describe the chemistry in an electrochemical cell and to find data for missing parameters needed in the modelling part.

3.2 Modelling procedure

Modelling of the membrane in the salt split cell is the main focus of the thesis. MATLAB ver.8 (R2012b) was used for this purpose. The cationic exchange membrane in a two compartment cell was modeled and some input data from previously conducted experiments at AkzoNobel was used.

Model development consists of different steps and often becomes an iterative procedure [18]. The procedure for the model development used in this thesis is shown in Figure 6, followed by a description of each step [18].

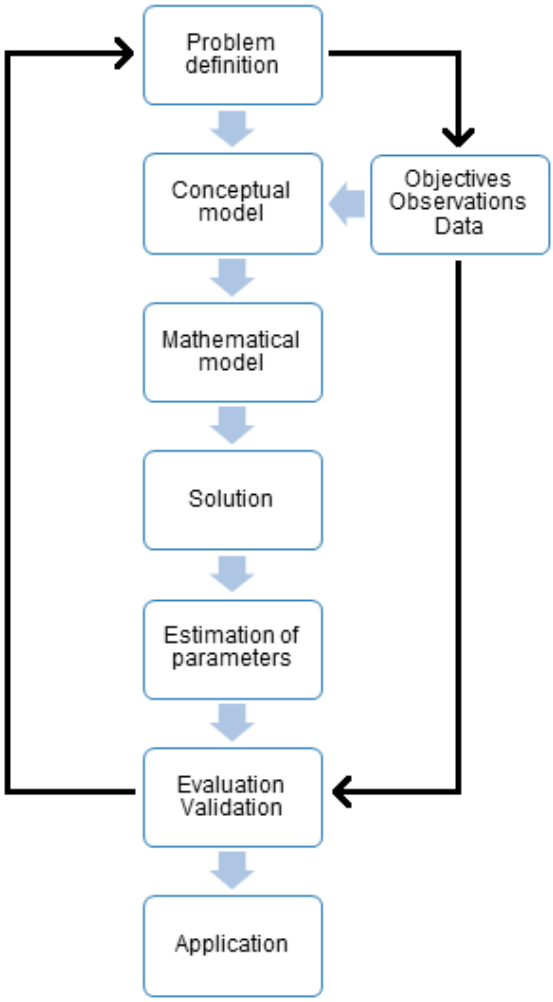

Figure 6: The procedure for model development, reproduced from [18].

The problem was defined by stating clear goals for the modelling. The derived model should be able to answer the research questions that are stated in the thesis.

Formulation of the conceptual model was done in order to identify governing physical and chemical principles, as well as underlying mechanisms. Decisions were made on what hypothesis and assumptions are to include. Also data and knowledge about the relevant topic, i.e. electrolysis with ion transport through a membrane, was gathered for the formulation of the conceptual model.

Formulation of the mathematical model was done by representing important quantities with a suitable mathematical entity, for example by a variable. Independent and dependent variables were specified, as well as relevant parameters. In this case, independent variables are defined as the variable being changed. Dependent variables are the ones being observed due to the change. Parameters can either be constants or a function of other variables.

Constraints or limitations for the variables were identified, by for example appropriate magnitude and range. Boundary conditions, i.e. what relations that are valid at the

systems boundaries, and initial conditions for the time-dependent equations were specified.

When the mathematical problem is solved, the validity of individual relationships was checked. Analytical solution was compared with numerical solution. Also the mathematical solution was verified by ensuring that the equations are solved correctly, by considering the residuals.

Parameters were determined, either by constant values or values from the laboratory setup. However, some parameters used in the model had to be estimated.

If the model has inadequacies, it has to be modified by an iterative process, see black arrows in Figure 6, which was done when adding boundary layers near the membrane into the model. For evaluation of the model and how output is affected by uncertainties in the parameter value of boundary layer thickness, sensitivity analysis was performed.

After validation and evaluation, the model is ready to be applied for the defined purpose.

3.3 Solution methods

When modelling the transport of ions together with the equation for the potential, the equations must first be classified in order to choose the appropriate solution method. The derived equations are parabolic second-order non-linear partial differential equations (PDEs). Therefore the built-in PDE solver in MATLAB, *pdepe*, is chosen. It solves initial-boundary value problems for system of PDEs that are parabolic or elliptic, in space variable x and in time t [23]. A restriction of the *pdepe*-solver is that at least one of the PDEs in the system must be parabolic [23]. Since the complete Nernst-Planck equation is coupled with the equation for the potential, these must be solved simultaneously. This is done by defining a system of PDEs.

The *pdepe*-solver converts the PDEs into ordinary differential equations (ODEs) [23]. This is done by a second-order accurate spatial discretization which is based on fixed set of specified nodes. For the time integration, the multistep *ode15s*-solver of variable-order is used [23]. Then both the formula and the time step are changed dynamically [23]. The *ode15s*-solver is based on numerical differentiation formulas (NDFs) and it can solve differential-algebraic equations that arise from elliptic equations [24]. *Ode15s* is also able to solve stiff problems where multiple time scales are present, otherwise causing abrupt fluctuations in the data series [18].

If assuming no accumulation, i.e. no variation of a certain quantity in time, the partial differential equation (PDE) can be simplified to an ordinary differential equation (ODE) with only one independent variable [18]. When solving second-order ODEs in MATLAB they must first be converted into a system of two first-order ODEs [24]. The ODE can be classified either as an initial-value problem (IVP) or as a boundary-value problem (BVP) [18].

For a boundary value problem the built-in BVP solver in MATLAB, *bvp4c*, is used. The *bvp4c*-solver uses a finite difference code where the three-stage *Lobatto IIIa* collection formula is applied and gives a fourth-order accurate solution [25]. To solve the BVP an initial guess of boundary values on the space interval are needed to be specified for the required solution [25]. The mesh selection and error control is determined from the residuals of the continuous numerical solution at each subinterval.

3.3.1 Finite difference method

The finite difference method (FDM) or control volume method (CVM) can be used to solve the governing equations for the transport of ions described by the Nernst-Planck equation.

The central difference for first-order differentials are [7]:

$$\left.\frac{\mathrm{d}c_i}{\mathrm{d}x}\right|_j = \frac{c_i(j+1)-c_i(j-1)}{2h} + O(h^2) \tag{33}$$

This introduces an error of order h^2 which can be minimized by smaller nodes, i.e. mesh interval h successively extrapolating to the correct solution. Plotting the answer against h^2 should yield a straight line on linear scales [7].

For second-order differentials, the central differences are [7]:

$$\left.\frac{\mathrm{d}^2c_i}{\mathrm{d}x^2}\right|_j = \frac{c_i(j+1)+c_i(j-1)-2c_i(j)}{h^2} + O(h^2) \tag{34}$$

3.3.2 Boundary and initial conditions

When developing mathematical models and solving the derived differential equations, appropriate boundary conditions and/or initial conditions are needed. The set of conditions specifies certain values a solution must take at its boundary and for boundary conditions three types can be used [18]:

- *Dirichlet* – specifies the value, example $y(0) = \gamma_1$
- *Neumann* – specifies the value of the derivative, example $\left.\frac{\partial y}{\partial x}\right|_{x=0} = \gamma_1$
- *Robin* – specifies a linear combination of the function and its derivative, example $a_1 y + b_1 \left.\frac{\partial y}{\partial x}\right|_{x=0} = \gamma_1$

In this thesis, only *Dirichlet* boundary conditions are specified for the ionic concentrations and electric potential at the left and right side of the membrane.

3.4 Experimental setup

The experimental setup is described, both to get additional understanding for the salt splitting process and to understand the background for the previously obtained data.

The lab setup is already built and available for use at AkzoNobel in Bohus. The electrochemical cell is a modified MP-cell (ElectroCell A/S, Denmark) with a zero gap configuration on the anode side of the cell. The zero gap is due to higher flow rate, and thus higher pressure, in the cathode compartment which essentially presses the membrane onto the anode.

The cell includes two electrodes (anode and cathode), one membrane, six gaskets and two spacers, see Figure 7. The anode is a DSA (Dimension Stable Anode) made of titanium with oxygen formation coating and the cathode is made of nickel. The projected area of each electrode is 100 cm^2 and the electrodes are surrounded by 1 mm thick gaskets made of EPDM rubber. The Nafion 324 bi-layer membrane is in total 152.4 μm thick and the electrode distance is about 2 mm. The main layer of the membrane towards the anolyte is 127 μm with an equivalent weight (EW) of 1100 g/mol and on the cathode side there is a barrier layer of 25.4 μm with equivalent weight 1500 g/mol [6]. The inflow and outflow of the anolyte respectively catholyte is at the short side of the spacers, which are placed outside of the electrodes. The spacers are meshed to promote the mixing and turbulence of the electrolytes.

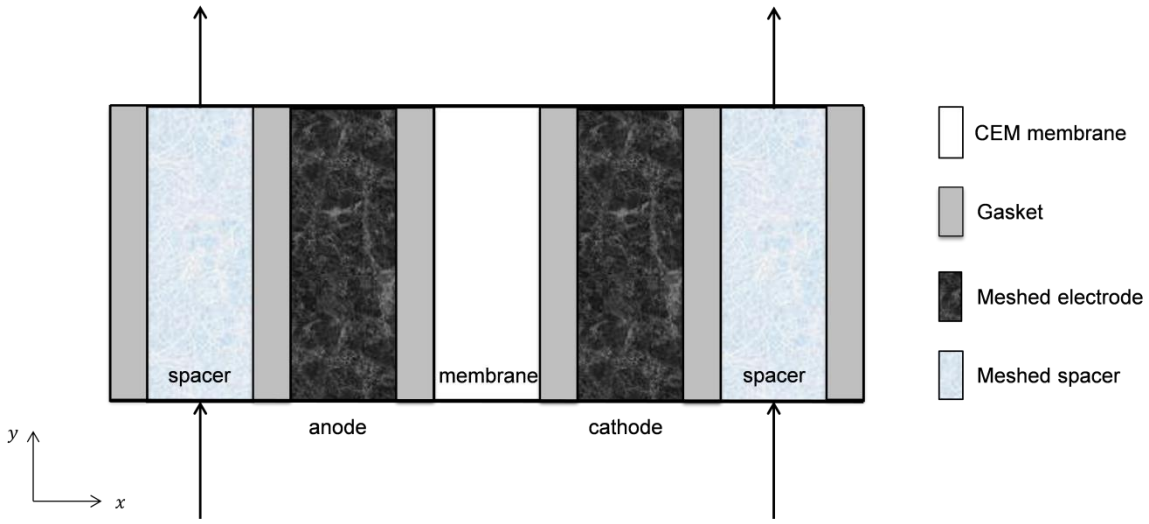

Figure 7: Structure of the electrochemical cell (not according to dimension).

A rectifier is controlling the current and the voltage is measured over the electrodes. There are instruments to measure the pressure before the cell. In a typical case, the cell voltage is 4.2 V and the pressure difference is 0.14 bar. The voltage drop over the membrane is 10% of the cell voltage [15], i.e. 0.42 V. The current density is 3.5 kA/m^2 and the operating temperature is set to 80˚C.

3.5 Modelling parameters

The constant parameters that are used in the modelling are shown in Table 1.

Table 1: Constant parameters used in the modelling.

Parameter	**Value**
Valence number, z_{Na^+}	1
Valence number, z_{H^+}	1
Valence number, z_{OH^-}	-1
Faraday's constant, F [A·s/mol]	96485
Ideal gas constant, R [J/K·mol]	8.3144621
Temperature, T [K]	353.15
Vacuum permittivity, ε_0 [F/m]	$8.85419 \cdot 10^{-12}$

The parameters that vary in different layers are presented in Table 2. Data for several of the parameters was not found for the N324-membrane, thus literature values for other similar Nafion membranes (N117, N115) were used. The N117-membrane is a perfluorosulfonic acid CEM with the same equivalent weight as the first layer sulfonate layer as in N324.

Table 2: Variable parameters for different layers and membrane.

Parameter	**Anolyte boundary layer**	**Membrane**	**Catholyte boundary layer**
Diffusivity, D_{Na^+} [m^2/s]	$1.11 \cdot 10^{-9}$ [26]	$0.98 \cdot 10^{-10}$ (N117) [5]	$1.11 \cdot 10^{-9}$ [26]
Diffusivity, D_{H^+} [m^2/s]	$3.33 \cdot 10^{-9}$*	$3.5 \cdot 10^{-10}$ (N117) [5]	$3.33 \cdot 10^{-9}$*
Diffusivity, D_{OH^-} [m^2/s]	$4.43 \cdot 10^{-9}$ [26]	$1.6 \cdot 10^{-11}$ (N324) [27]	$4.43 \cdot 10^{-9}$ [26]
Diffusivity, D_{H_2O} [m^2/s]		$9 \cdot 10^{-10}$ (N115) [28]	
Thickness of layers, L [m]	$0/10 \cdot 10^{-6}$* /$50 \cdot 10^{-6}$*	$152.4 \cdot 10^{-6}$ (=$127 \cdot 10^{-6}$+$25.3 \cdot 10^{-6}$)	$0/10 \cdot 10^{-6}$* /$50 \cdot 10^{-6}$*
Potential drop, $\Delta\Phi$ [V]	0/0.001155/0.005776 [Appendix B.1]	0.42	0/0.0005073/0.002536 [Appendix B.1]
Relative permittivity, ε_r	39.59 [Appendix B.2]	20 (N117) [10, 29]	54.81 [Appendix B.2]

* *Estimated values for the boundary layers.*

Due to lack of accurate information of the flow properties outside of the membrane surface, for example in terms of the Reynolds number, it is difficult to estimate the boundary layer thickness. Three different values, from zero to 50 μm, are chosen for the film thickness. The potential drop for the different boundary layers is calculated by using Ohm's law and estimated values for the conductivity, see Appendix B.1 for calculations. The relative permittivity for the boundary layers is approximated from the water permittivity, see Appendix B.2.

The membrane is assumed to be homogenously populated with fixed sites and the modelling is done without considering the ion channels in nanoscale or any molecular interactions. Also the membrane is modelled as one layer, but with existence of reliable parameters and values for ion diffusivity coefficients in the two layers of Nafion 324 the model would be straight forward to use.

Parameters that are used to calculate the velocity of species through the membrane is presented in Table 3. The dynamic viscosity is in this case an approximation of the anolyte solution, consisting of 21 wt.-% Na_2SO_4 and 14 wt.-% H_2SO_4. The direction for the ion transport is defined positive from the anolyte compartment towards the catholyte compartment. Due to a higher pressure in the catholyte than in the anolyte, the velocity will have a negative value. For detailed calculations of the velocity, see Appendix B.3.

Table 3: Parameters used for calculating velocity through the membrane.

Parameter	**Value**
Porosity, ϕ	0.25 (N117) [30]
Permeability, k [m^2]	$7.13 \cdot 10^{-20}$ (N115) [11]
Dynamic viscosity, μ [Pa·s]	$0.5 \cdot 10^{-3}$ (AkzoNobel's database)
Pressure drop, ΔP [bar]	0.14 (lab setup)
Velocity, v [m/s]	$-5.2399 \cdot 10^{-13}$ [Appendix B.3]

3.5.1 Modelling boundary and initial conditions

The boundary values for the concentrations of the species and electric potential is shown in Table 4. The concentration of sodium ions is obtained from measurements in the lab setup, as well as for hydroxyl ions in the cathode compartment. The hydroxyl concentration in the anolyte compartment is assumed to be zero, since it is very acidic there ($pH = -0.11$). The boundary concentrations of hydrogen ions are calculated, see Appendix B.4. For boundary values for the potential there is no information and therefore an arbitrary value is chosen at the anolyte side of the membrane, in this case half of the cell voltage, and the other boundary is determined by the specified potential drop over the membrane. When adding film layers, the calculated potential drops

presented in Table 2 for the different layers are added to or subtracted from the boundary values of the potential.

Table 4: Boundary values used in modelling.

Parameter	**Anolyte**	**Catholyte**
Sodium, c_{Na^+} [M]	3.842 (lab setup)	2.74 (lab setup)
Hydrogen ion, c_{H^+} [M]	1.5473 [Appendix B.4]	$3.7154 \cdot 10^{-12}$ [Appendix B.4]
Hydroxyl, c_{OH^-} [M]	0	2.74 (lab setup)
Water, c_{H_2O} [M]	45.5893	53.7722
Potential, Φ [V]	2.1+ $\Delta\Phi_{anolyte\ layer}$	1.68- $\Delta\Phi_{catholyte\ layer}$

Estimated initial conditions for both the membrane and electrolytes in the boundary layers are shown in Table 5. Before installation in the electrochemical splitting cell, the membrane is placed in 1 wt.-% $NaOH$.

Table 5: Initial conditions used in modelling.

Parameter	**Anolyte**	**Membrane**	**Catholyte**
Sodium, c_{Na^+} [M]	4.256	0.2	0
Hydrogen ion, c_{H^+} [M]	0	0	0
Hydroxyl, c_{OH^-} [M]	0	0.2	0
Potential, Φ_m [V]	0	0	0

3.6 Modelling settings

For the numerical solutions, some setting values are presented in Table 6.

Table 6: Setting values used in modelling.

Setting	**Value in BVP**	**Value in PDE**
Mesh nodes	3000	200
Relative residual	10^{-9}	10^{-3}
Absolute residual	10^{-12}	10^{-6}

4 Results and Discussion

In this section the modelling of transport phenomena through the membrane is presented, by using the Nernst-Planck equation for the ion transport together with the Laplace condition for the electrical potential. First the model equations are simplified and then the solution is obtained by simulations in form of profiles, followed by discussion after each part. Lastly, some model limitations are discussed.

4.1 Model simplification

Model simplification is done by reducing the number of dimensions in the geometry and by reducing the number of independent variables in the modelling equations.

The model is further simplified by investigating what terms in the equation that are significant. This is done by comparing the terms describing the ion transport in the Nernst-Planck equation and determining what mechanisms are the most important for ion transport through the membrane.

4.1.1 Dimensions and independent variables

The complete Nernst-Planck equation is a function of time and space and is given in vectorial form as:

$$\frac{\partial c_i}{\partial t} = D_i \nabla^2 c_i + \frac{z_i F D_i}{RT} \nabla c_i \nabla \Phi - v \nabla c_i \tag{9}$$

Assuming transport in one direction through the membrane only, i.e. the transport of ions from the anolyte to the catholyte, the equation is simplified to (the x-direction is normal to the membrane):

$$\frac{\partial c_i(x,t)}{\partial t} = D_i \frac{\partial^2 c_i(x,t)}{\partial x^2} + \frac{z_i F D_i}{RT} \frac{\partial c_i(x,t)}{\partial x} \frac{\mathrm{d}\Phi(x,t)}{\mathrm{d}x} - v \frac{\partial c_i(x,t)}{\partial x} \tag{35}$$

The direction in this thesis will always be positive from the anolyte compartment towards the catholyte compartment.

The partial differentials, ∂, is approximated with the ordinary differentials, d, when solving the equation as a boundary-value problem:

$$\frac{\mathrm{d}c_i(t)}{\mathrm{d}t} = D_i \frac{\mathrm{d}^2 c_i(x)}{\mathrm{d}x^2} + \frac{z_i F D_i}{RT} \frac{\mathrm{d}c_i(x)}{\mathrm{d}x} \frac{\mathrm{d}\Phi(x)}{\mathrm{d}x} - v \frac{\mathrm{d}c_i(x)}{\mathrm{d}x} \tag{36}$$

The same simplification is done for the Laplace condition on the potential, where the general equation is given first, and then written in one dimension and finally without the partial differential:

$$\nabla^2 \Phi = 0 \tag{32}$$

$$\frac{\partial^2 \Phi(x,t)}{\partial x^2} = 0 \tag{37}$$

$$\frac{\mathrm{d}^2 \Phi(x)}{\mathrm{d}x^2} = 0 \tag{38}$$

4.1.2 Convection vs diffusion term

Comparison between the convection term and the diffusion term from Nernst-Planck equation is done by creating a ratio in the dimensionless form:

$$convection = v\frac{\mathrm{d}c_i}{\mathrm{d}x} \approx v\frac{\Delta c}{\Delta x} \approx v\left(-\frac{C}{L}\right)$$

$$diffusion = D_i\frac{\mathrm{d}^2c_i}{\mathrm{d}x^2} \approx D_i\frac{\Delta c}{(\Delta x)^2} \approx D_i\frac{C}{L^2}$$

$$ratio_{C/D} = \frac{convection}{diffusion} = \frac{v\left(-\frac{C}{L}\right)}{D_i\frac{C}{L^2}} = -\frac{vL}{D_i} = dim.less \tag{39}$$

This dimensionless ratio between the convection and diffusion term can be found in the literature as the Peclet number [17, 18].

If $ratio_{C/D} \ll 1$ → Total flux ≈ diffusional flux

If $ratio_{C/D} \approx 1$ → Total flux = diffusional flux + convectional flux

If $ratio_{C/D} \gg 1$ → Total flux ≈ convectional flux

Inserting values for the parameters and the values for the diffusivity coefficients for each of the ions, into equation (39), gives the ratios:

$$ratio_{C/D} = -\frac{vL}{D_i} = \begin{Bmatrix} D_i = D_{Na^+} \\ D_i = D_{H^+} \\ D_i = D_{OH^-} \end{Bmatrix} = \begin{matrix} 8.1486 \cdot 10^{-7} \\ 2.2816 \cdot 10^{-7} \\ 4.9910 \cdot 10^{-6} \end{matrix}$$

It can be concluded that the diffusion term completely dominates for all cases, and thus the convection term can be excluded.

4.1.3 Migration vs diffusion term

A comparison between the migration term and the diffusion term from Nernst-Planck equation is done by creating a ratio in the dimensionless form:

$$migration = \frac{z_iFD_i}{RT}\frac{\mathrm{d}\Phi}{\mathrm{d}x}\frac{\mathrm{d}c_i}{\mathrm{d}x} \approx \frac{z_iFD_i}{RT}\frac{\mathrm{d}\Phi}{\mathrm{d}x}\frac{\Delta c}{\Delta x} \approx \frac{z_iFD_i}{RT}\frac{\mathrm{d}\Phi}{\mathrm{d}x}\left(-\frac{C}{L}\right)$$

$$diffusion = D_i\frac{\mathrm{d}^2c_i}{\mathrm{d}x^2} \approx D_i\frac{\Delta c}{(\Delta x)^2} \approx D_i\frac{C}{L^2}$$

$$ratio_{M/D} = \frac{migration}{diffusion} = \frac{\frac{z_iFD_i\mathrm{d}\Phi}{RT\ \mathrm{d}x}\left(-\frac{C}{L}\right)}{D_i\frac{C}{L^2}} = -\frac{z_iF\frac{\mathrm{d}\Phi}{\mathrm{d}x}L}{RT} = dim.less \tag{40}$$

If $ratio_{M/D} \ll 1$ → Total flux ≈ diffusional flux

If $ratio_{M/D} \approx 1$ → Total flux = diffusional flux + migrational flux

If $ratio_{M/D} \gg 1$ → Total flux ≈ migrational flux

The derivative for the potential is assumed to be constant and calculated by using values at the anolyte side and the catholyte side of the membrane:

$$\frac{\mathrm{d}\Phi}{\mathrm{d}x} = \frac{\Phi_{\mathrm{cat}} - \Phi_{\mathrm{an}}}{L} \approx \frac{\Delta\Phi}{L}$$

Inserting this together with the other parameters, into equation (40) gives the ratio:

$$ratio_{M/D} = -\frac{z_i F \Delta\Phi}{RT} = 68.9988$$

Since the ratio is larger than 1 the migration term for the Nernst-Planck equation dominates. However, since the ratio should be several orders of magnitudes larger to safely remove a term in order to simplify a model [18], the diffusion term is kept in the model.

Varying the potential at the anolyte side of the membrane from a really low value to maximal value, $\Phi_{\mathrm{an}} = (0.42 : 4.2)$, and assuming the potential drop to 10%, gives the $ratio = (14 : 138)$. This indicates that migration term will be only one ten potential to maximum two ten potentials larger than the diffusion term. Thus it is reasonable to keep both terms in the model for ion transport.

4.1.4 Migration vs convection term

Comparing the migration term and the convection term from Nernst-Planck equation is done by creating a ratio in the dimensionless form:

$$migration = \frac{z_i F D_i}{RT}\frac{\mathrm{d}\Phi}{\mathrm{d}x}\frac{\mathrm{d}c_i}{\mathrm{d}x} \approx \frac{z_i F D_i}{RT}\frac{\mathrm{d}\Phi}{\mathrm{d}x}\frac{\Delta c}{\Delta x} \approx \frac{z_i F D_i}{RT}\frac{\mathrm{d}\Phi}{\mathrm{d}x}\left(-\frac{C}{L}\right)$$

$$convection = v\frac{\mathrm{d}c_i}{\mathrm{d}x} \approx v\frac{\Delta c}{\Delta x} \approx v\left(-\frac{C}{L}\right)$$

$$ratio_{M/C} = \frac{migration}{convection} = \frac{\frac{z_i F D_i}{RT}\frac{\mathrm{d}\Phi}{\mathrm{d}x}\left(-\frac{C}{L}\right)}{v\left(-\frac{C}{L}\right)} = \frac{z_i F D_i \frac{\mathrm{d}\Phi}{\mathrm{d}x}}{RTv} = dim.less \qquad (41)$$

If $ratio_{M/C} \ll 1$ → Total flux ≈ convectional flux

If $ratio_{M/C} \approx 1$ → Total flux = convectional + migrational flux

If $ratio_{M/C} \gg 1$ → Total flux ≈ migrational flux

The derivative for the potential is assumed to be constant and calculated by using values at the anolyte side and the catholyte side of the membrane:

$$\frac{\mathrm{d}\Phi}{\mathrm{d}x} = \frac{\Phi_{\mathrm{cat}} - \Phi_{\mathrm{an}}}{L} \approx \frac{\Delta\Phi}{L}$$

Inserting this together with the other parameters and the values for the diffusivity coefficients for each of the ions, into equation (41), gives the ratios:

$$ratio_{M/C} = \frac{z_i F D_i \Delta\Phi}{RTvL} = \begin{Bmatrix} D_i = D_{Na^+} \\ D_i = D_{H^+} \\ D_i = D_{OH^-} \end{Bmatrix} = \begin{matrix} 8.4676 \cdot 10^7 \\ 3.0241 \cdot 10^8 \\ 1.3825 \cdot 10^7 \end{matrix}$$

The migration term dominates for all cases with several orders of magnitude, and thus the convection term can be excluded. This can of course also be concluded directly from the comparisons above.

4.1.5 Final simplified model

The Nernst-Planck ion transport model after the afore-mentioned simplifications is:

$$\frac{\mathrm{d}c_i}{\mathrm{d}t} = D_i \frac{\mathrm{d}^2 c_i}{\mathrm{d}x^2} + \frac{z_i F D_i}{RT} \frac{\mathrm{d}c_i}{\mathrm{d}x} \frac{\mathrm{d}\Phi}{\mathrm{d}x} \tag{42}$$

For some of the solution approaches steady-state is assumed.

4.2 Solution structure of model equations

The final simplified Nernst-Planck model, equation (42), for the ion transport is solved for the ion concentrations with three approaches; analytical solution of BVP, numerical solution of BVP and numerical solution of PDE. The resulting solution structure of these approaches is described in this section, followed by some profiles obtained from the solutions in Sections 4.3-4.6.

4.2.1 Analytical solution of BVP

The analytical solution for Nernst-Planck equation with Laplace condition for the electrical potential, i.e. constant potential drop across the membrane, at steady state is presented:

$$0 = D_i \frac{\mathrm{d}^2 c_i}{\mathrm{d}x^2} + \frac{z_i F D_i}{RT} \frac{\Delta\Phi}{\Delta \mathrm{x}} \frac{\mathrm{d}c_i}{\mathrm{d}x} \tag{43}$$

$$0 = \frac{\mathrm{d}^2 c_i}{\mathrm{d}x^2} + \frac{z_i F \Delta\Phi}{RT\mathrm{L}} \frac{\mathrm{d}c_i}{\mathrm{d}x} \tag{44}$$

Using $y = c_i(x)$ and $a = \frac{z_i F \Delta\Phi}{RT\mathrm{L}}$, a homogeneous equation is obtained:

$$y'' + ay' = 0 \tag{45}$$

This is classified as a second-order linear ordinary differential equation and the auxiliary equation to the homogeneous equation is then:

$$r^2 + ar = 0 \tag{46}$$

With the distinct real roots being:

$$r_1 = 0$$

$$r_2 = -a$$

Two solutions are obtained from these roots as follows:

$$y_1 = e^{r_1 x} = 1 \tag{47}$$

$$y_2 = e^{r_2 x} = e^{-ax} \tag{48}$$

The general solution is then:

$$y = Ay_1 + By_2 = A + Be^{-ax} \tag{49}$$

Where A and B are arbitrary constants, which can be determined by initial conditions:

$$y(0) = c_1 \quad \Rightarrow \quad A + B \cdot 1 = c_1$$

$$y(L) = c_2 \quad \Rightarrow \quad A + Be^{-aL} = c_2$$

This gives new values for the constants:

$$A = c_1 - \frac{c_2 - c_1}{e^{-aL} - 1} \tag{50}$$

$$B = \frac{c_2 - c_1}{e^{-aL} - 1} \tag{51}$$

The final analytical solution of the second-order boundary-value problem is:

$$y = c_1 - \frac{c_2 - c_1}{e^{-aL} - 1} + \frac{c_2 - c_1}{e^{-aL} - 1} e^{-ax} \tag{52}$$

$$y = c_1 + \frac{c_2 - c_1}{e^{-aL} - 1}(e^{-ax} - 1) \tag{53}$$

Written with the original variables, the analytical solution is:

$$c_i(x) = c_1 + \frac{c_2 - c_1}{e^{-\frac{z_i F \Delta\Phi}{RTL} L} - 1}\left(e^{-\frac{z_i F \Delta\Phi}{RTL} x} - 1\right) \tag{54}$$

4.2.2 Numerical solution of BVP

To solve the Nernst-Planck equation (42) and Laplace equation (38) for the potential as boundary-value problems in MATLAB, functions for the BVP and its boundary conditions are formulated. Firstly, steady state, $\frac{\mathrm{d}c_i}{\mathrm{d}t} = 0$, for the Nernst-Planck equation is assumed which gives:

$$\frac{\mathrm{d}^2 c_i}{\mathrm{d}x^2} = -\frac{z_i F}{RT} \frac{\mathrm{d}c_i}{\mathrm{d}x} \frac{\mathrm{d}\Phi}{\mathrm{d}x} \tag{55}$$

This equation must be solved for each species, with the additional relation for potential distribution:

$$\frac{\mathrm{d}^2 \Phi}{\mathrm{d}x^2} = 0 \tag{38}$$

The second-order differential equations are rewritten as a system of two first-order differential equations to be able to solve them as a boundary-value problem with the MATLAB *bvp4c*-solver:

$$y_1 = c_i(x)$$

$$\mathrm{y}_2 = \frac{\mathrm{d}y_1}{\mathrm{d}x}\left(= \frac{\mathrm{d}c_i}{\mathrm{d}x}\right)$$

$$\frac{\mathrm{d}y_2}{\mathrm{d}x} = \frac{z_i F}{RT} \mathrm{y}_2 \frac{\mathrm{d}\Phi}{\mathrm{d}x} \left(= \frac{\mathrm{d}^2 c_i}{\mathrm{d}x^2} \right)$$

$$y_3 = \Phi(x)$$

$$y_4 = \frac{\mathrm{d}y_3}{\mathrm{d}x} \left(= \frac{\mathrm{d}\Phi}{\mathrm{d}x} \right)$$

$$\frac{\mathrm{d}y_4}{\mathrm{d}x} = 0 \left(= \frac{\mathrm{d}^2 \Phi}{\mathrm{d}x^2} \right)$$

Written in the ODE-function in the following form:

$$dydx = \begin{bmatrix} y_2 \\ \frac{z_i F}{RT} \mathrm{y}_2 y_4 \\ y_4 \\ 0 \end{bmatrix}$$

Dirichlet left and right boundary conditions, bc_l and bc_r, for the functions are specified at the interval boundaries x_0 and x_f:

$$bc = \begin{bmatrix} y_1(\mathrm{x}_0) - bc_l(c_i) \\ y_1(\mathrm{x}_\mathrm{f}) - bc_r(c_i) \\ y_3(\mathrm{x}_0) - bc_l(\Phi) \\ y_3(\mathrm{x}_\mathrm{f}) - bc_r(\Phi) \end{bmatrix}$$

The MATLAB-code used for the numerical solution is presented in Appendix D.

4.2.3 Numerical solution of PDE

When solving partial differential equations in the MATLAB *pdepe*-solver, functions for the PDE, initial conditions and the boundary conditions are formulated. The Nernst-Planck PDE (42) and equation for the Laplace PDE (38) potential are solved simultaneously and rewritten accordingly:

$$u_1 = c_i(x,t)$$

$$u_2 = \Phi(x,t)$$

$$\begin{bmatrix} 1 \\ 0 \end{bmatrix} \cdot \frac{\partial}{\partial t} \begin{bmatrix} u_1 \\ u_2 \end{bmatrix} = \frac{\partial}{\partial x} \cdot \begin{bmatrix} D_i \frac{\mathrm{d}u_1}{\mathrm{d}x} + \frac{z_i F D_i}{RT} u_1 \frac{\mathrm{d}u_2}{\mathrm{d}x} \\ \frac{\mathrm{d}u_2}{\mathrm{d}x} \end{bmatrix} + \begin{bmatrix} 0 \\ 0 \end{bmatrix}$$

Initial conditions, ic, for both the concentration and potential are specified:

$$u0 = \begin{bmatrix} ic(c_i) \\ ic(\Phi) \end{bmatrix}$$

Dirichlet values for the left and right boundary conditions, bc_l and bc_r, are specified in the following form:

$$\begin{bmatrix} u_1 - bc_l(c_i) \\ u_2 - bc_l(\Phi) \end{bmatrix} + \begin{bmatrix} 0 \\ 0 \end{bmatrix} \cdot \begin{bmatrix} \frac{\mathrm{d}u_1}{\mathrm{d}x} \\ \frac{\mathrm{d}u_2}{\mathrm{d}x} \end{bmatrix} = \begin{bmatrix} 0 \\ 0 \end{bmatrix}$$

$$\begin{bmatrix} u_1 - bc_r(c_i) \\ u_2 - bc_r(\Phi) \end{bmatrix} + \begin{bmatrix} 0 \\ 0 \end{bmatrix} \cdot \begin{bmatrix} \frac{\mathrm{d}u_1}{\mathrm{d}x} \\ \frac{\mathrm{d}u_2}{\mathrm{d}x} \end{bmatrix} = \begin{bmatrix} 0 \\ 0 \end{bmatrix}$$

The MATLAB-code used for the numerical solution is presented in Appendix E.

4.3 Concentration and flux profiles

The concentration and flux profiles of sodium ions, hydrogen ions and hydroxyl ions through the membrane are shown in Figure 8, Figure 9 and Figure 10, respectively.

The concentration profiles are obtained from the analytical solution of BVP, numerical solution of BVP and numerical solution of PDE. For the numerical solution of PDE, the concentration profile for the ions from the last time iteration is used. The complete surface profiles of the PDE solution are shown in Appendix F.

The flux profile is obtained from equation (5), with same model simplifications as described in Section 4.1, by using the cation concentrations and its derivatives together with the derivative from the potential, from the numerical solution of the BVP.

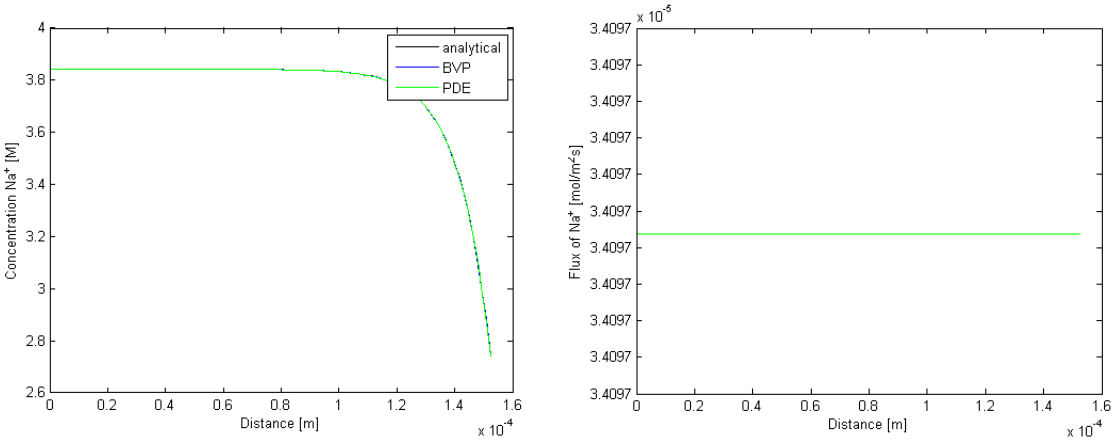

Figure 8: Concentration profile for sodium ions in the membrane from analytical, BVP and PDE solution (in the left plot) and flux profile from BVP solution (in the right plot).

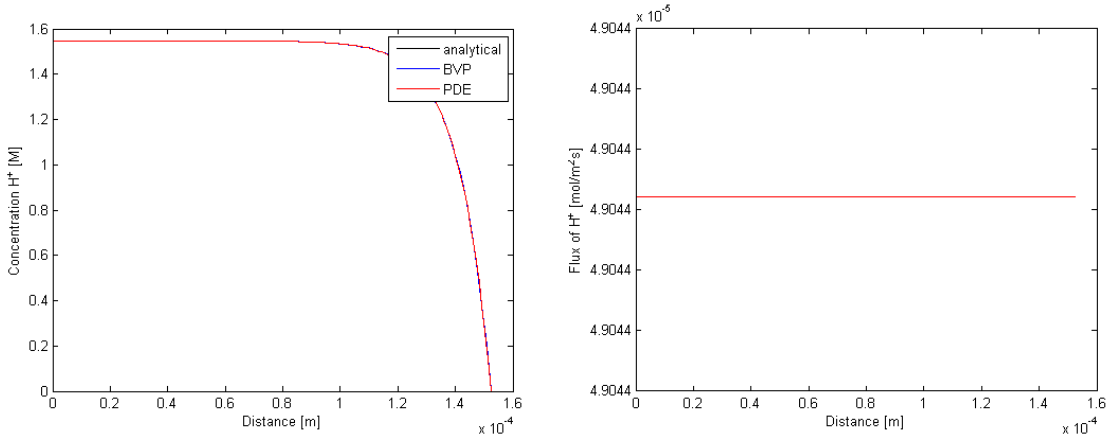

Figure 9: Concentration profile for hydrogen ions in the membrane from analytical, BVP and PDE solution (in the left plot) and flux profile from BVP solution (in the right plot).

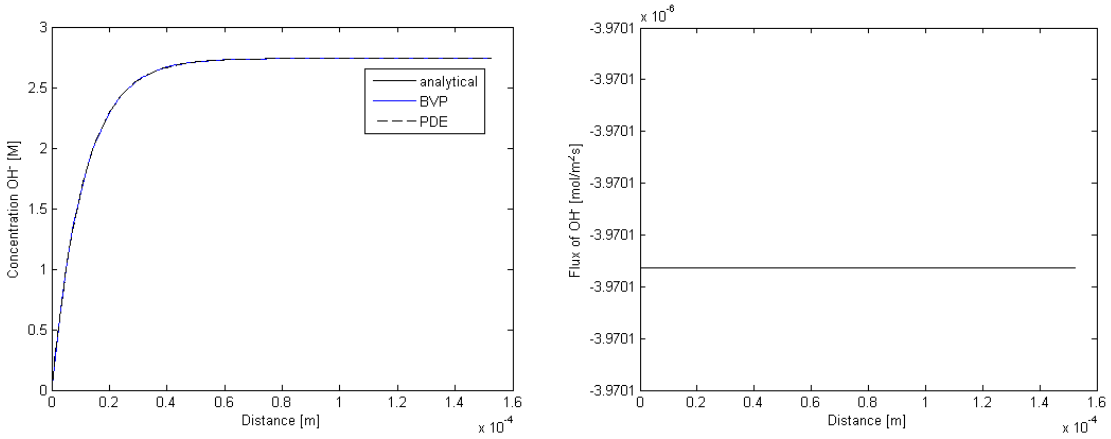

Figure 10: Concentration profile for hydroxyl ions in the membrane from analytical, BVP and PDE solution (in the left plot) and flux profile from BVP solution (in the right plot).

All concentration profiles from the numerical solutions, BVP and PDE, resemble the analytical solution. From the concentration profiles for both sodium ions and hydrogen ions, it can be seen that the concentration decrease through the membrane, from the anolyte side to the catholyte side. This is expected since there is a concentration difference across the membrane for the ions, with higher concentration at the anolyte side. The profiles show that the decrease starts in the middle of the membrane and is largest towards the end of the membrane. Important to point out is that the solution is obtained by specifying the boundary values, so the solution is affected by these. Also, it is important to remember that the sodium ions compete for the fixed sites in the membrane with hydrogen ions, affecting the current efficiency.

The profile of hydroxyl ions is mirrored to the cations profiles. Even though the membrane is considered to be in acidic state, the transport of hydroxyl ions is simulated, which can be further investigated, if relevant. All hydroxyl ions should be neutralized at the right boundary side of the membrane in the case of the acid membrane state, as described in Section 2.1.2.

From all the flux profiles it can be seen that the flux of ions is constant through the entire membrane, which indicates that the flux into the membrane is equal to the flux out of the membrane. This seems reasonable considering the steady-state assumption. Comparing the fluxes, it can be seen that the flux of hydrogen ions is a bit higher than the sodium ion flux. This can possibly be explained by that hydrogen ions are smaller, and have a higher diffusivity, than sodium ions and thus transport of hydrogen ions through the membrane is favored. Both cations have a positive value of the flux throughout the membrane, while hydroxyl ions have a negative value, which is expected. This means that the transport of hydroxyl ions occurs in opposite direction i.e. from the catholyte compartment to the anolyte compartment.

4.4 pH profile

The pH profile, obtained from the concentration of hydrogen ions from the analytical solution, numerical solution of BVP and numerical solution of PDE, is shown in Figure 11.

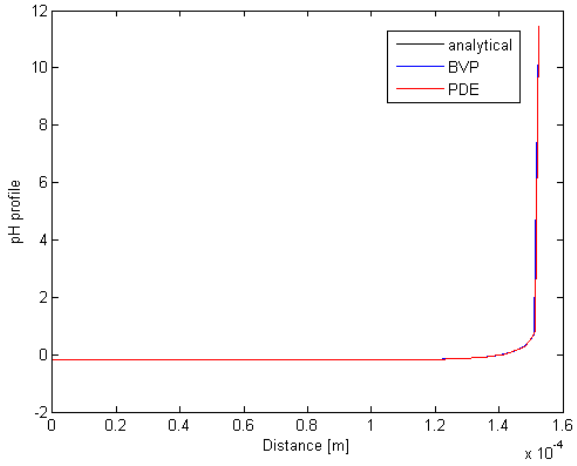

Figure 11: pH profile in the membrane from analytical, BVP and PDE solution.

As can be seen from all the concentration profiles for the hydrogen ion, most of the change happens towards the catholyte side of the membrane and thus the same is seen for the pH profile. The solution is once again highly dependent on the boundary values specified.

4.5 Electric potential profile

The profile for the electric potential from the BVP solution and PDE solution is shown in Figure 12.

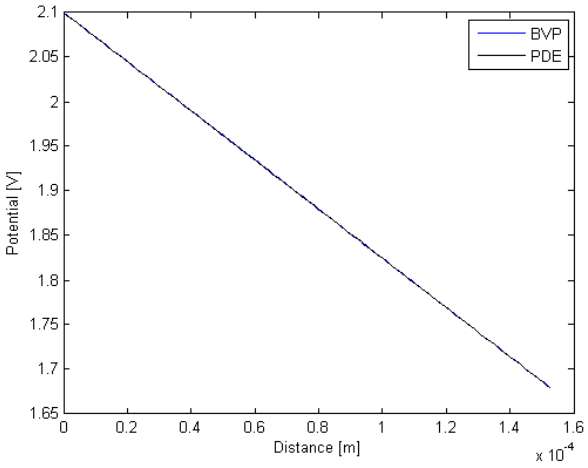

Figure 12: Electric potential profile in the membrane from BVP solution and PDE solution.

As expected from the Laplace expression of the second-order differential equation for the electric potential, the profile is a straight line with constant slope between set boundary values. Even if the values for the potential were not known at the boundaries, the important parameter is the potential drop across the layer of interest in the model equation for the ion transport. For the analytical solution the potential drop is assumed constant, and thus the profile would then look like the potential profiles shown in Figure 12.

4.6 Water transport

For water transport, the transport number due to electro-osmosis and hydrated ions is used and the profile is seen in Figure 13.

The flux profile for water is obtained from equation (17) together with equation (5), with same model simplifications as described in Section 4.1, by using the cation concentrations and its derivatives together with the derivative of the potential, from the numerical solution of the BVP.

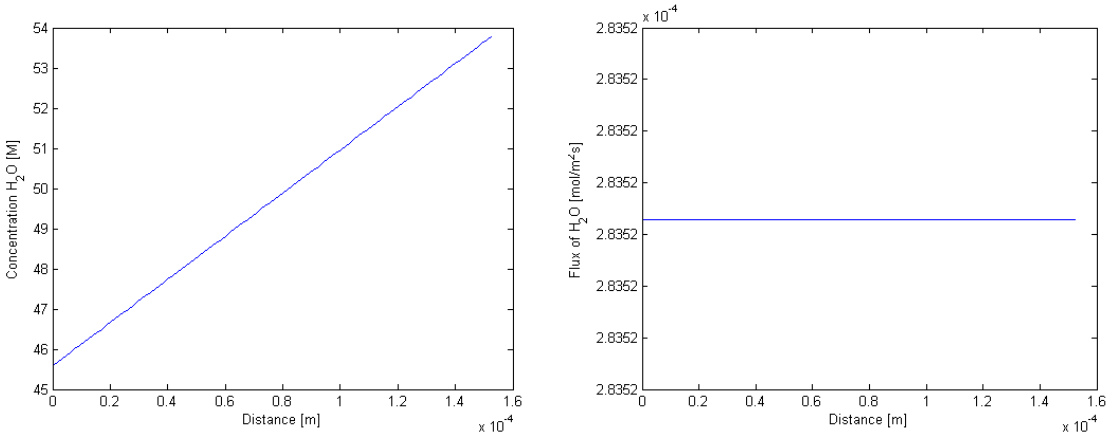

Figure 13: Concentration profile for water in the membrane from BVP solution (in the left plot) and flux profile from BVP solution (in the right plot)

The water transport through the membrane is considered to be large by looking at the profiles from the BVP solution, compared to the ion concentration and flux profiles in Section 4.3. This is expected since the defined water transport is due to electro-osmosis and transport of hydrated ions. The ion-exchange membrane easily lets the cations through thus water is transported as well.

Swelling of membrane due to contact with water changes the thickness of the membrane and this can also affect the ion transport.

4.7 Boundary layers

For profiles through the membrane with boundary layers, the same numerical solution structure with PDEs as described in Section 4.2.3, when only modelling the membrane, is used. To account for the different layers, different diffusion coefficients are specified, see Section 3.5. Since the profiles through the membrane in Section 4.3 are very similar, difference on the fourth decimal at the curves of the profiles, only the PDE solution is shown from now on by changing the boundary layer thickness in the MATLAB-code shown in Appendix E.

4.7.1 Concentration profiles

The concentration profile from the last time iteration of sodium ions, hydrogen ions and hydroxyl ions through the membrane is shown in Figure 14, Figure 15 and Figure 16, respectively.

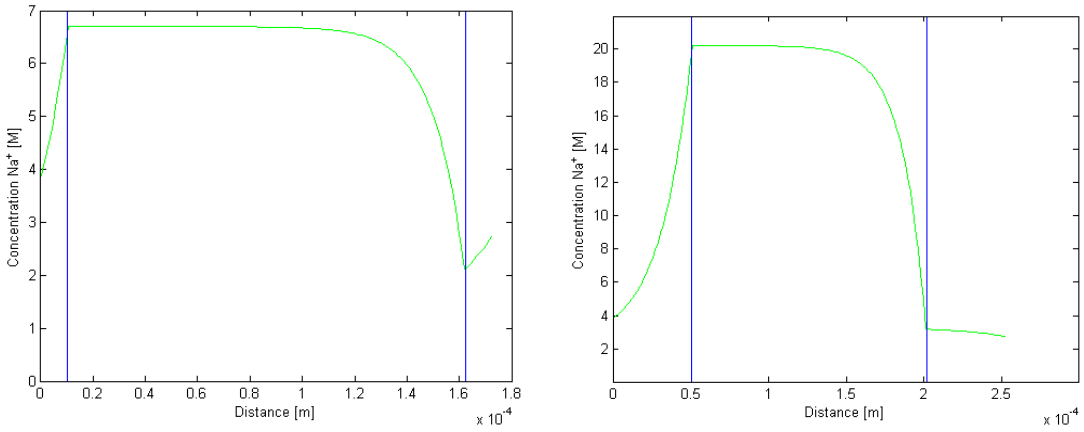

Figure 14: Concentration profile for sodium ions in the membrane and boundary layers, 10 µm (in the left plot) and 50 µm (in the right plot), from PDE solution.

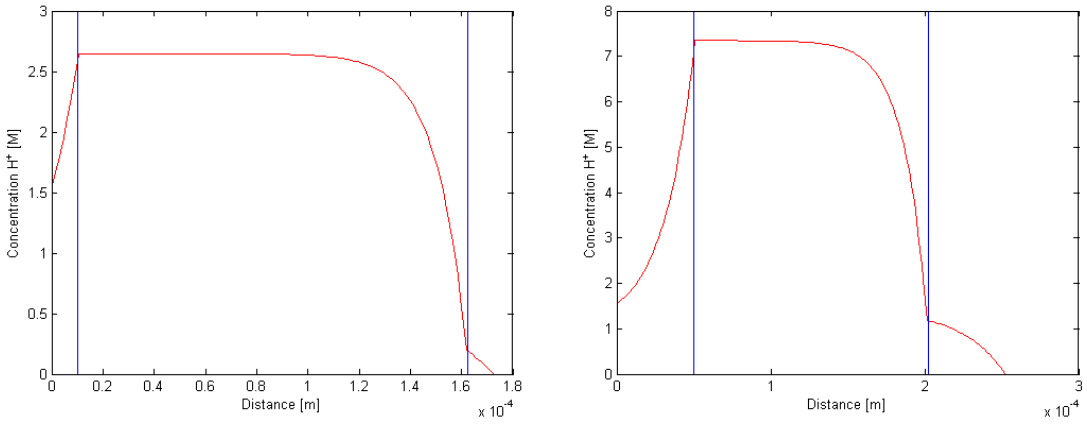

Figure 15: Concentration profile for hydrogen ions in the membrane and boundary layers, 10 µm (in the left plot) and 50 µm (in the right plot), from PDE solution.

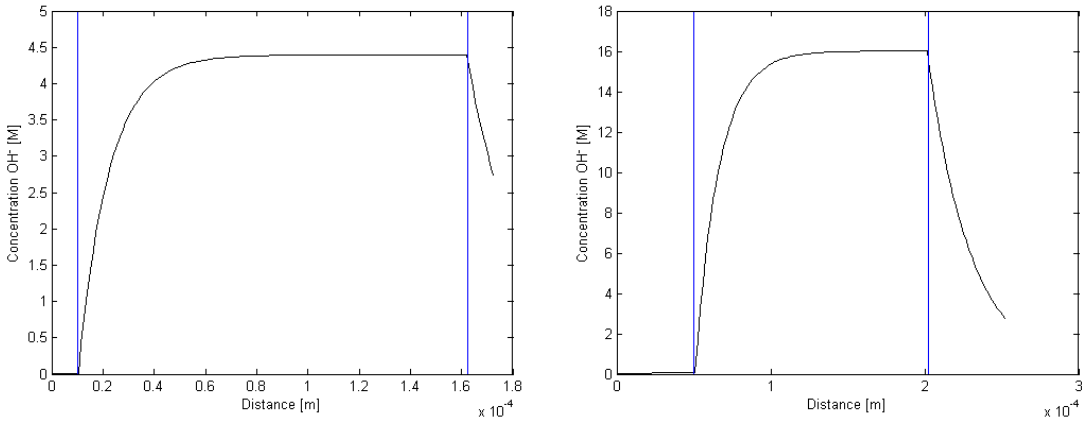

Figure 16: Concentration profile for hydroxyl ions in the membrane and boundary layers, 10 µm (in the left plot) and 50 µm (in the right plot), from PDE solution.

When comparing the resulting plots with different thicknesses, it can be seen that the concentration profile for the ions have the same shape through the membrane even if boundary layers are added. However the magnitude of the profiles varies considerably, i.e. the wider the boundary layer thickness, the higher the concentration of ions inside the membrane. If the film is made thinner than 10 µm, the profile will have a lower increase in the anolyte boundary layer and if the film thickness is made thicker than 50 µm, the profile will have a higher increase in the anolyte boundary layer compared to the concentrations profiles shown above. This observation does not have an obvious explanation. Intuitively, the concentration profile would decrease towards the membrane surface and a wider boundary layer thickness would lead to lower concentration at the surface of the membrane.

4.7.2 pH profile

The pH profile through the membrane and boundary layers, obtained from the concentration of hydrogen ions, is shown in Figure 17.

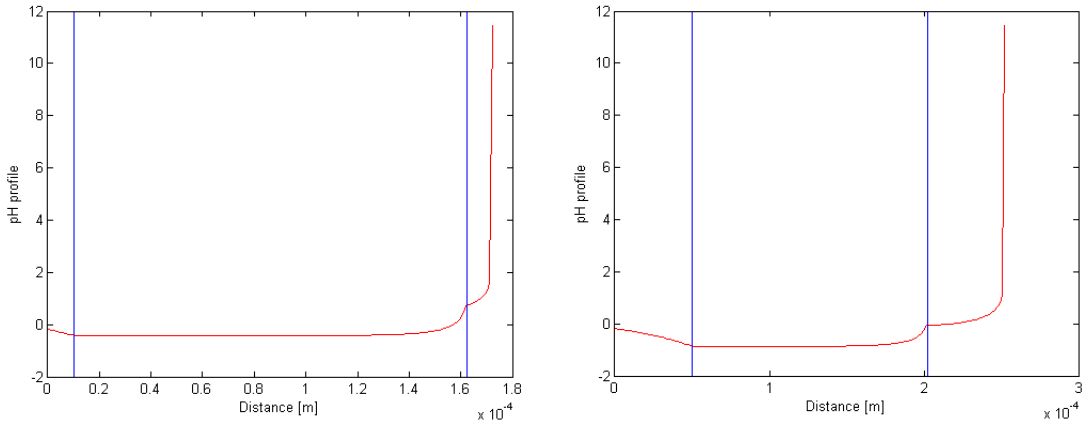

Figure 17: pH profile in the membrane and boundary layers, 10 µm (in the left plot) and 50 µm (in the right plot), from PDE solution.

When adding boundary layers, the alkaline pH values ($pH > 7$) are reached in the second boundary layer in the catholyte compartment rather than inside the membrane when only the membrane is modelled with bulk values as boundary conditions (see Figure 11). This result in Figure 17 is favorable since the existence of precipitations, which can occur at high pH due to impurities inside the electrochemical cell, can be avoided.

4.7.3 Electric potential profile

The profile for the electric potential through the membrane and boundary layers is shown in Figure 18.

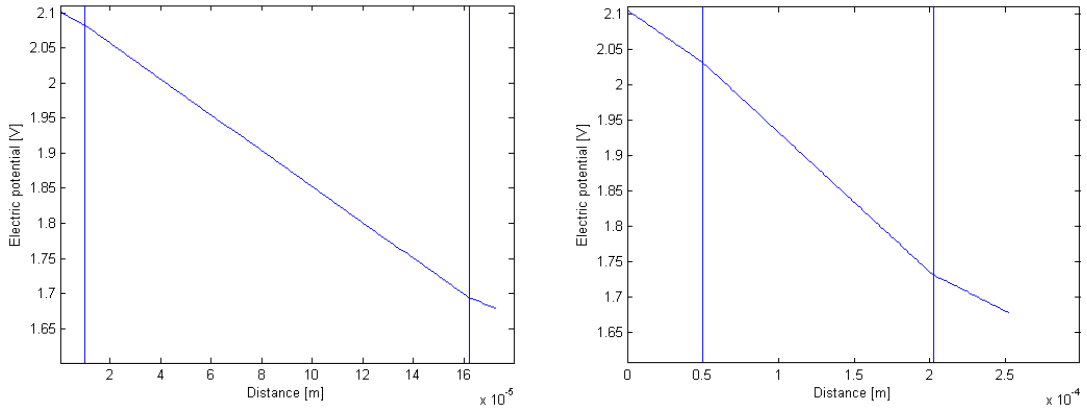

Figure 18: Electric potential profile in the membrane and boundary layers, 10 µm (in the left plot) and 50 µm (in the right plot), from PDE solution.

The potential drop in the boundary layers is smaller than in the membrane, due to higher conductivity and lower resistance in the solutions. Also the relative permittivity is higher in the solution than in the membrane, leading to smaller potential drop. It can however be seen that there is a slightly higher slope for the potential drops in the boundary layers in Figure 18 compared to the calculated values in Table 2. It cannot be

explained why the numerical solver do not interpret the specified condition properly. Attempts have been made with both solvers, BVP and PDE, however without success. It is though possible to obtain a profile with proper slopes of the electrical potential by specifying intermediate boundary conditions on the length interval, but this approach then requires boundary conditions for the concentrations as well, which is not present.

4.8 Influence of impurities

Impurities of other cations in the anolyte and catholyte can influence the desired transport of the sodium ions. In a cation exchange membrane with fixed negative sulfonate acid groups (SO_3^-), the counter-ion exchange sequence is [8]:

$$Ba^{2+} > Pb^{2+} > Sr^{2+} > Ca^{2+} > Mg^{2+} > Ag^{+} > K^{+} > NH^{4+} > Na^{+} > Li^{+}$$

Considering the counter-ion exchange sequence, this indicates that larger monovalent cations than sodium ions or multivalent ions have larger affinity to the negatively charged fixed sulfonate groups in the interior of the membrane. Intuitively, this will affect the desired sodium transport negatively by decreasing the current efficiency. Also based on the pH, the presence of impurities can lead to precipitations inside or on the surface of the membrane.

However, how impurities specifically affect the transport through the membrane was not investigated in the thesis, mostly because of lack of data for the diffusivities in the membrane. Also molecular interactions can occur, especially for non-dilute solutions, and thus affect the transport of ions. Incorporation of this effect into the model is not straight forward since multicomponent diffusivities are needed which are difficult to obtain.

4.9 Model limitations

The conceptual modelling and mathematical equations were presented in Chapter 2, the parameter estimation was presented in Chapter 3 and the solutions of the modelling equations were presented in this chapter. The validity of the model was verified by using very low residuals, fine mesh size for the length dimension and time step intervals being changed dynamically by the numerical solvers. Evaluation of the model parameters, which should be done with independent measurements, is not performed in the thesis. Lack of data for several of the parameters is a large factor when assessing the quality of the model. In the present results, most membrane specific parameters are missing for the Nafion 324 membrane. Even though appropriate estimates are made, it is important to emphasize that the parameters could be completely different and thus significantly different results could be expected.

The derived model based on the Nernst-Planck equation is limited to dilute solutions and the activity coefficients are assumed to unity, which may not be the case and can thus influence the result. Probably the modified Nernst-Planck equation presented in Appendix A could be used to cope with this.

4.9.1 Model simplifications

When considering the mass conservation law, all transport mechanisms should be included in a model describing the transport. However, the simplification of the model when the convection term is neglected is very reasonable since the membrane is considered to be very compact and the calculated velocity is very small. Of course any damage of the membrane can lead to pinholes and thus significant convection of species through the membrane can occur, but this is not considered during normal operation. Also for the boundary layers, the convection term can safely be neglected when comparing with the other terms, diffusion and migration, with several orders of magnitude to spare. This holds even if the diffusivity coefficients in the solvents are one order of magnitude larger than in the membrane.

The geometry and dimensional simplification also is considered appropriate, since flow into the cell is spread out by the meshed spacers and thus the length is probably not influencing the bulk values considerably. This effect however could be significant if the dimensions of the cell are much larger and the spacers do not have the capability to spread out the flow evenly.

Steady state models are far more usable and relevant than any type of dynamic models as the typical operation is steady operation and the operational changes resulting in time dependent parameters can be fully neglected over time. For this reason it is sufficient to use the BVP modelling approach. Comparing the plots from the PDE solution with the BVP solution, they are very similar and the graphs almost coincide after some computational time.

4.9.2 Influence of bi-layer membrane

In the thesis a mono-layer membrane layer is modelled, even if the N324-membrane in reality is a bi-layer membrane. If relevant parameters were known the model can easily be extended to modelling of the bi-layer membrane. Considering the bi-layer membrane, the second layer towards the catholyte side has a higher equivalent weight which means that the reactivity of the polymer is lower than in the first layer, as well as lower hydraulic permeability. There are less active sites in the second layer making it harder for the ions to go through and thus a protection against the catholyte. Based on this, the diffusivities of ions are probably lower in the second layer compared to the diffusivity coefficients in the first membrane layer. The concentration profile through the membrane would then most likely decrease even further towards the cathode side of the membrane.

4.9.3 Electric potential and electro-neutrality

The Laplace expression for the electric potential was derived by the assumption of electro-neutrality, which is considered as an appropriate assumption both for the solution in the boundary layers and also through the membrane.

The Laplace condition on the electric potential may however not be appropriate close to the interface between the membrane and the boundary layers, where a charged double layer with cations can build up. This is because the fixed negative charges on the membrane surface creates an electric field which attracts cations from the solution, thus creating a layer close to the surface of the membrane where the concentration of cations is higher than in the bulk solution [8]. Because of the possibly charged double layer at the interface between the boundary layers and the membrane, the electro-neutrality assumption would probably not hold here. This charged layer is though extremely small, some molecule diameters wide (about 10^{-10} m), so probably the effect can be neglected or handled by incorporating some interface relations.

Limitation of the Laplace condition on the electric potential is also present close to electrodes where very strong electric fields are present, leading to separation of charges and thus no electro-neutrality.

4.9.4 Boundary layers close to membrane

The focus of the modelling has been on the transport of ions through the membrane, but even if the flow regime inside the two compartments in the electrochemical cell is considered turbulent due to gas evolution at the electrodes and presence of meshed spacers, there is probably a thin laminar boundary layer at the surface of the membrane. It is important to remember that the same model equations were used in all layers and the only parameters that differed were the diffusivity coefficients, permittivity and the potential drop. The same parameter values for the diffusivity coefficients and layer thickness in the two boundary layers were used, which is probably not the case in reality. The ionic diffusivity coefficients are dependent on the concentration of the solution [7]. Due to a higher flow rate of the catholyte, the boundary layer on the catholyte side of the membrane should probably be thinner than the boundary layer thickness on the anolyte side of the membrane.

4.9.5 Flow phase of electrolytes

In the current model, the multiphase flow nature of the electrolyte is neglected. This assumption is supposed to be acceptable in cells where gas evolution occurs at the surface of the electrodes typically placed outside of the electrolytes. Then the electrolyte close to the boundary layers should not be affected considerably because of the cell design. However, when the electrolyte is placed outside of the electrodes instead, as in the electrochemical cell described in this thesis, the gas evolution might have an effect on the bulk concentrations and thus the results. The effect of multiphase flows is however not incorporated in the modelling and this is not investigated in the thesis. It is believed that single phase modelling is sufficient for this case since the bulk concentration should not be affected significantly when the electrolyte is considered well mixed.

4.9.6 Experimental validation

The derived model can only be used in this specific case with the particular experimental set for the parameters and boundary values. Nothing can be said for the application of the model in other ranges of the parameters. To cope with this, independent experiments and comparison to other experimental data is needed. Validation of the model can also be done with reference to literature data for other similar modelling cases. These approaches are however not done in the thesis and remain for completing the modelling procedure.

5 Conclusions

It can be concluded that the objectives with the thesis are met. A model for the transport through the membrane has been derived and solved. Thereby the understanding of the transport phenomena and parameters relevant for the ion-exchange membrane in a sodium sulfate electrochemical splitting cell has been significantly clarified.

The model equation, with the dominating migration and diffusion terms, describes the ion transport through the membrane after some simplifications. The main parameters for the modelling are found to be the bulk concentrations, for the boundary conditions, and diffusivities for the ions. Also potential drop, permittivity and thickness of film layers are important. The rest of the parameters are constants or membrane specifications. The following conclusions can be made from this study:

- The numerical solutions with the two approaches, BVP and PDE, give very similar results as the analytical solution of the model equation, when modelling the transport of sodium ions, hydroxyl ions and hydrogen ions through the membrane. The profile for the electric potential is a straight line with constant slope, as expected from the Laplace condition of the potential.
- Water transport through the membrane is highly affected by the cation concentration because the main water transport is due to electro-osmosis together with transport of ions having hydrated shells. For this case the transport number was found to be important for modelling of the water transport.
- The pH profile show very low acidic values in the anolyte and alkaline values in the catholyte. The location where the transition occurs is found to depend on the boundary layer thickness. Also, the ionic concentration profiles depend on the thickness of the boundary layer and it can be concluded that wider boundary layer thicknesses give higher concentrations of ions inside the membrane.
- Impurities with larger or multivalent cations will affect the transport of the desired sodium ions through the membrane negatively, when considering the counter-ion exchange sequence.

For the modelling procedure, verification of the mathematical solution by comparing the solution with formerly obtained results, is not performed due to lack of such results. Also experimental validation of the models remains. However, the derived model and code is ready for use in MATLAB for further investigation.

6 Future Work

Due to time constraints, several aspects of the modelling remain which can be further improved. In the present stage of modelling the transport of ions through the Nafion 324 membrane, there are many unknown parameters. Hopefully, the results from the estimated parameters until this point can give proper profiles, trends and indications, but further work is needed for a more correct and detailed model. The following work would be recommended:

- Modify the modelling equation to non-dilute case by adding a concentration dependent factor in the expression for chemical potential.
- Make new estimates for modelling parameters by experimental measurements.
- Validate the model by independent experimental results, if possible.
- Ensure good model quality by considering accuracy, descriptive realism, precision, robustness, generality and fruitfulness.
- Sensitivity analysis for additional parameters with uncertainties.
- Compare modelling results by using different modelling programs.
- Consider other description levels of modelling, for example molecular scale.
- Investigate if gas evolution at the electrodes is affecting the results by modelling the electrolytes as multiphase flows.

References

[1] F. Öhman, L. Delin, N. Simic and K. Pelin, "Electrolysis of sodium sulphate - efficient use of salt cake and ESP dust in pulp mills," ÅF Industry & AkzoNobel PPC, 2014.

[2] H. Vogt, J. Balej, J. E. Bennett, P. Wintzer, S. Akbar Sheikh, P. Gallone and K. Pelin, "Chlorine Oxides and Clorine Oxygen Acids," in *Ullmann's Encyclopedia of Industrial Chemistry*, Weinheim, Wiley-VCH Verlag, 2010.

[3] G. Ranger, "A review of selected electrochemical technologies to manage chlorine dioxide generator saltcake production and its conversion to useful chemicals," *Journal of Science & Technology for Forest Products and Processes,* vol. 3, no. 4, pp. 13-18, 2013.

[4] J. Jörissen and K. H. Simmerock, "The behaviour of ion exchange membranes in electrolysis and electrodialysis of sodium sulphate," *Journal of Applied Electrochemistry,* vol. 21, no. 10, pp. 869-876, 1991.

[5] M. Rakib, P. Mocotéguy, P. Viers, E. Petit and G. Durand, "Behaviour of Nafion 350 membrane in sodium sulfate electrochemical splitting: continuous process modelling and pilot scale tests," *Journal of Applied Electrochemistry,* vol. 29, no. 12, pp. 1439-1448, 1999.

[6] W. Grot, Fluorinated Ionomers, Oxford: Elsevier Inc., 2011.

[7] J. Newman and K. E. Thomas-Alyea, Electrochemical Systems, Hoboken: John Wiley & Sons, Inc., 2004.

[8] H. Strathmann, Ion-Exchange Membrane Separation Processes, Amsterdam: Elsevier B.V., 2004.

[9] Nafion Bulletin 98-04, "Nafion N-324," DuPont Product Information.

[10] S. A. Schmidt, "Mathematical models of ion transport through nafion membranes in modified electrodes and fuel cells without electroneutrality," PhD thesis, University of Iowa, 2010.

[11] Q. Duan, H. Wang and J. Benziger, "Transport of liquid water through Nafion membranes," *Journal of Membrane Science,* Vols. 392-393, pp. 88-94, 2012.

[12] T. Tjärnhage, "Thin Polymer and Phospholipid Films for Biosensors: Characterisation with Gravimetric, Electrochemical and Optical Methods," PhD thesis, Umeå University, 1996.

[13] S. M. Davis, G. E. Gray and P. A. Kohl, "Candidate membranes for the

electrochemical salt-splitting of Sodium Sulfate," *Journal of Applied Electrochemistry,* vol. 38, no. 6, pp. 777-783, 2008.

[14] M. Paleologou, A. Thibault, P.-Y. Wong, R. Thompson and R. M. Berry, "Enhancement of the current efficiency for sodium hydroxide production from sodium sulphate in a two-compartment bipolar membrane electrodialysis system," *Separation and Purification Technology,* vol. 11, pp. 159-171, 1997.

[15] Nafion Bulletin 95-01, "Voltage Effects in Membrane Chloralkali Cells," DuPont Technical Information.

[16] M. J. Cheah, I. G. Kevrekidis and J. Benziger, "Effect of interfacial water transport resistance on coupled proton and water transport across nafion," *The Journal of Physical Chemistry B,* vol. 115, pp. 10239-10250, 2011.

[17] J. R. Welty, C. E. Wicks, R. E. Wilson and G. L. Rorrer, Fundamentals of Momentum, Heat, and Mass Transfer, Hoboken: John Wiley & Sons, 2008.

[18] A. Rasmuson, B. Andersson, L. Olsson and R. Andersson, Mathematical Modeling in Chemical Engineering - model formulation, simplification and validation, Gothenburg: Chalmers University, 2013.

[19] T. A. Davis, J. D. Genders and D. Pletcher, A First Course in Ion Permeable Membranes, Hants: The Electrchemical Consultancy, 1997.

[20] S. Psaltis, "Multicomponent Charge Transport in Electrolyte Solutions," PhD thesis, Queensland University of Technology, 2012.

[21] N. Tzanetakis, W. M. Taama and K. Scott, "Salt Splitting in a Three-compartment membrane Electrolysis Cell," *Filtration+Separation,* vol. 39, no. 3, pp. 30-38, 2002.

[22] K. Krabbenhøft and J. Krabbenhøft, "Application of the Poisson-Nernst-Planck equations to the migration test," *Cement and Concrete Research,* vol. 38, pp. 77-88, 2008.

[23] MathWorks-Documentation, "Partial Differential Equations," The MathWorks, Inc, [Online]. Available: http://uk.mathworks.com/help/matlab/math/partial-differential-equations.html. [Accessed 27 Mars 2015].

[24] MathWorks-Documentation, "Ordinary Differential Equation," The MathWorks, Inc, [Online]. Available: http://uk.mathworks.com/help/matlab/math/ordinary-differential-equations.html. [Accessed 19 Mars 2015].

[25] MathWorks-Documentation, "Boundary-Value Problems," The MathWorks, Inc., [Online]. Available: http://uk.mathworks.com/help/matlab/math/boundary-value-

problems.html. [Accessed 19 Mars 2015].

[26] P. Bosander, G. Sundström and E. Fontes, AkzoNobel, internal report, 1999.

[27] S. M. Davis, "Electrochemical splitting of sodium sulfate," MSc Thesis, Georgia Institute of Technology, 2006.

[28] S. Motupally, A. J. Becker and J. W. Weidner, "Diffusion of Water in Nafion 115 Membranes," *Journal of The Electrochemical Society,* vol. 147, no. 9, pp. 3171-3177, 2000.

[29] S. J. Paddison, D. W. Reagor and T. A. J. Zawodzinski, "High Frequency Dielectric Studies of Hydrated Nafion," *Journal of Electroanalytical Chemistry,* vol. 459, pp. 91-97, 1998.

[30] M. W. Verbrugge and R. F. Hill, "Experimental and Theoretical Investigation of Perfluorosulfonic Acid Membranes Equilibrated with Aqueous Sulfuric Acid Solutions," *The Journal of Physical Chemistry,* vol. 92, no. 23, pp. 6778-6783, 1988.

[31] M. W. Verbrugge, E. W. Schneider, R. S. Conell and R. F. Hill, "The effect of temperature on the equilibrium and transport properties of saturated poly(perfluorosulfonic acid) membranes," *Journal of Electrochemical Society,* vol. 139, no. 12, pp. 3421-3428, 1992.

[32] E. Fontes, AkzoNobel, internal report, 1997.

[33] A. K. Sahu, S. Pitchumani, P. Sridhar and A. K. Shukla, "Nafion and modified-Nafion membranes for polymer electrolyte fuel cells: An overview," *Bulletin of Material Science,* vol. 32, no. 3, pp. 285-294, 2009.

A Modified Nernst-Planck Equation

Using the electrochemical potential as driving force and Nernst-Einstein relation for the mobility, the Nernst-Planck equation becomes [7]:

$$N_i = -u_i c_i \nabla \mu_i + c_i v \tag{56}$$

$$N_i = -\frac{D_i c_i}{RT} \nabla \mu_i + c_i v \tag{57}$$

The gradient of the electric potential, $\nabla \mu_i$, which depends on the local electrical state and the local composition can be written as:

$$\nabla \mu_i = \nabla \left(\mu_i - \frac{z_i}{z_n} \mu_n \right) + \frac{z_i}{z_n} \nabla \mu_n \tag{58}$$

Where the quasi-electrostatic potential, μ_n, is defined as [7]:

$$\mu_n = RT \ln c_n + z_n F \Phi \tag{59}$$

The expression in the brackets in equation (58) can be written as:

$$\mu_i - \frac{z_i}{z_n} \mu_n = RT \left[\ln\left(\alpha_i^\theta c_i f_i\right) - \frac{z_i}{z_n} \ln\left(\alpha_n^\theta c_n f_n\right) \right] = RT \left(\ln \alpha_i^\theta - \frac{z_i}{z_n} \ln \alpha_n^\theta \right) + RT \left(\ln c_i - \frac{z_i}{z_n} \ln c_n \right) + RT \left(\ln f_i - \frac{z_i}{z_n} \ln f_n \right) \tag{60}$$

At constant temperature, equation (58) can be expressed as:

$$\nabla \mu_i = RT \nabla \ln c_i + z_n F \nabla \Phi + RT \nabla \left(\ln f_i - \frac{z_i}{z_n} \ln f_n \right) \tag{61}$$

Inserting equation (61) into (57), the flux expression becomes:

$$N_i = -\frac{z_i D_i F}{RT} c_i \nabla \Phi - D_i \nabla c_i - D_i c_i \nabla \left(\ln f_i - \frac{z_i}{z_n} \ln f_n \right) + c_i v \tag{62}$$

The ion activity coefficient, f_i, can then be expressed by:

$$f_{i,n} = \frac{f_i}{f_n^{z_i/z_n}} \tag{63}$$

So, the final expression for the modified Nernst-Planck equation for moderately diluted solution is [7]:

$$N_i = -\frac{z_i D_i F}{RT} c_i \nabla \Phi - D_i \nabla c_i - D_i c_i \nabla \ln f_{i,n} + c_i v \tag{64}$$

B Calculations of Parameters for Modelling

In this section the calculation for some of the parameters are presented.

B.1 Calculation of potential drop in boundary layers

The potential drops through the boundary layers can be calculated by the divergence of potential from Ohm´s law:

$$i = -\kappa \nabla \Phi \tag{28}$$

$$\Rightarrow \nabla \Phi = -\frac{i}{\kappa} \tag{65}$$

Where the current density and conductivities for different layers are:

$i = 3500\ A/m^2$

$\kappa_{anolyte} = 30.3\ S/m$ (10 wt.-% $NaOH$, 70 ˚C) (AkzoNobel's database)

$\kappa_{catholyte} = 69\ S/m$ (20.2 wt.-% Na_2SO_4 and 10 wt.-% H_2SO_4, 70 ˚C) (AkzoNobel's database)

Inserting these values into the expression for the divergence of potential, $\nabla\Phi$, and multiplying with the specific thickness of each layer, L, gives the potential difference $\Delta\Phi$ for the different layers:

$$\Delta\Phi = -\frac{i}{\kappa_{anolyte}} L \tag{66}$$

$$\Delta\Phi_{anolyte\ layer} = -\frac{i}{\kappa_{anolyte}} L = \begin{Bmatrix} L = 10\ \mu m \\ L = 50\ \mu m \end{Bmatrix} = \begin{matrix} -0.001155\ V \\ -0.005776\ V \end{matrix}$$

$$\Delta\Phi_{catholyte\ layer} = -\frac{i}{\kappa_{catholyte}} L = \begin{Bmatrix} L = 10\ \mu m \\ L = 50\ \mu m \end{Bmatrix} = \begin{matrix} -0.0005073\ V \\ -0.002536\ V \end{matrix}$$

The negative value of the potential difference, $\Delta\Phi$, indicates that it is a potential drop.

B.2 Calculation of permittivity for electrolytes

The permittivity for pure water [30]:

$\varepsilon_{r,H_2O} = 78$

The water permittivity shows temperature dependence according to following relation [31]:

$$\varepsilon_{r,H_2O}(T) = 87.836914 - 0.396351 \cdot T + 0.000745 \cdot T^2 \tag{67}$$

This is valid in the following temperature interval:

$$0 < T < 100^{\circ}C \tag{68}$$

For the salt split cell 80˚C is used, this gives the water permittivity:

$$\Rightarrow \varepsilon_{r,H_2O} = \{T = 80^{\circ}C\} = 60.8968$$

The anolyte contains 65 wt.-% water and the catholyte contains 90 wt.-% water, which gives following relative permittivity as an approximation for respective electrolyte:

$$\varepsilon_{r,anolyte} = 0.65 \cdot \varepsilon_{r,H_2O}(T = 80^{\circ}C) = 39.5829$$

$$\varepsilon_{r,catholyte} = 0.90 \cdot \varepsilon_{r,H_2O}(T = 80^{\circ}C) = 54.8071$$

B.3 Calculation of velocity through the membrane

The velocity through the membrane is calculated by dividing the flow from Darcy's equation with the porosity:

$$v = \frac{q}{\phi} \tag{22}$$

$$q = -\frac{k}{\mu}\frac{\partial P}{\partial x} \tag{21}$$

$$\Rightarrow\ v = -\frac{k}{\phi\mu}\frac{\Delta P}{L} \tag{69}$$

Where:

$k = 7.13 \cdot 10^{-20}\ m^2$ (N115) [11]

$\Delta P = 0.14\ bar$

$L = 152.4\ \mu m = 1.524 \cdot 10^{-4}\ m$

$\mu = 5 \cdot 10^{-4}\ Pa\ s$

$\phi = 0.25$ (N117) [30]

This gives the velocity through membrane:

$$\Rightarrow\ v = -5.2399 \cdot 10^{-13}\ m/s$$

B.4 Calculation of free acidity in electrolytes

The concentration of hydrogen ions, i.e. the free acidity, in the cathode compartment is calculated by an equation derived for solution of sodium sulfate and sulfuric acid [32]:

$$c_{H^+} = 0.41 \cdot \left(c_{H_2SO_4} + c_{Na_2SO_4}\right) \tag{70}$$

This equation is valid for the following ratio:

$$\frac{c_{H_2SO_4}}{c_{H_2SO_4} + c_{Na_2SO_4}} = 0.5 \tag{71}$$

Where:

$c_{H_2SO_4} = 1.853\ M$

$c_{Na_2SO_4} = 1.921\ M$

This gives the hydrogen ion concentration in the anolyte:

$$\Rightarrow\ c_{H^+} = 1.5473\ M$$

For the concentration of hydrogen ions in the cathode compartment, the measured pH-value is used:

$$pH = 11.43$$

$$c_{H^+} = \log_{10}(pH) \tag{72}$$

$$\Rightarrow c_{H^+} = 3.7154 \cdot 10^{-12}\ M$$

B.5 Calculation of sulfonate concentration in membrane

The concentration of the negatively charged sulfonate groups, c_S, is calculated by the specified equivalent weight of the two layers of the N324-membrane and assuming they have the same density as the similar membrane N117, accordingly:

$$c_S = \frac{\rho_m}{EW} \tag{73}$$

Where

$EW_1 = 1100\ g/mol$ (N324) [6]

$EW_2 = 1500\ g/mol$ (N324) [6]

$\rho_m = 1740\ g/dm^3$ (N117) [10]

$$\Rightarrow c_{S,1} = \frac{\rho_m}{EW_1} = \frac{1740\ g/dm^3}{1100\ g/mol} = 1.582\ M$$

$$\Rightarrow c_{S,2} = \frac{\rho_m}{EW_2} = \frac{1740\ g/dm^3}{1500\ g/mol} = 1.164\ M$$

C Peclet Number

The Peclet number is used to estimate what terms for mass transfer in the Nernst-Planck equation are significant to include in the modelling of the transport of ions through the membrane.

Thickness of the membrane:

$$L = 152.4\,\mu m = 1.524 \cdot 10^{-4}\,m$$

Diffusivities for ions through Nafion 117 [5]:

$$D_{Na^+} = 0.98 \cdot 10^{-10} m^2/s$$

$$D_{H^+} = 3.5 \cdot 10^{-10}\,m^2/s$$

Both the molecular flux and convective flux are significant when $Pe \approx 1$. Assuming that $Pe = 1$, the velocity through the membrane is calculated from the Peclet equation:

$$Pe = \frac{vL}{D_i} \tag{74}$$

$$\Rightarrow \quad v = \frac{Pe \cdot D_i}{L} \tag{75}$$

$$v_{Na^+} = -6.43 \cdot 10^{-7}\,m/s$$

$$v_{H^+} = -2.30 \cdot 10^{-6}\,m/s$$

These velocities are considered very small and it is important to emphasize that the pressure gradient is opposite to the concentration gradient, i.e. there is a high concentration of cations in the anode compartment however the pressure is higher in the cathode compartment. The convective transports due to pressure difference will thus counteract against the diffusion of cations through the membrane and the velocity will therefore have a negative value.

From the calculated velocity, the permeability constant can be calculated by using Darcy's law. This limiting k can be compared with permeability for other membranes to determine if both diffusion flux and convection should be considered.

$$q = -\frac{k}{\mu}\frac{\partial P}{\partial x} \tag{21}$$

$$\Rightarrow \quad k = -\frac{q\mu\Delta x}{\Delta P} \tag{76}$$

The pressure difference over the membrane:

$\Delta P = 0.14\,bar$ (lab setup)

$\Delta x = L = 152.4\,\mu m = 1.524 \cdot 10^{-4}\,m$ (N324)

$\mu = 5 \cdot 10^{-4}\,Pa\,s$ (21 wt.-% Na_2SO_4 and 14 wt.-% H_2SO_4, 80 ˚C) (AkzoNobel's database)

$\phi = 0.25$ (N117) [30]

$$v = \frac{q}{\phi} \tag{22}$$

$$\Rightarrow \quad q = v\phi \tag{77}$$

Flow through membrane for the ions:

$$q_{Na^+} = -1.61 \cdot 10^{-7}\ m/s$$

$$q_{H^+} = -5.74 \cdot 10^{-7}\ m/s$$

The permeability for the limiting value of Pe can be calculated:

$$k = -\frac{q\mu\Delta x}{\Delta P} \tag{76}$$

$$k_{Na^+} = 8.75 \cdot 10^{-14}\ m^2$$

$$k_{H^+} = 3.13 \cdot 10^{-13}\ m^2$$

Permeability for Nafion N115 from literature [11]:

$$k = 7.13 \cdot 10^{-20}\ m^2$$

It can be seen that the calculated limiting permeability is much larger, order of magnitude 10^7, than the permeability found in the literature. For the permeability from literature, the Peclet number is:

$$\Rightarrow Pe = 8.8729 \cdot 10^{-8}$$

This Pe number is much smaller than 1, indicating that the convective flux can be neglected in comparison to the diffusional flux.

D MATLAB-code for Modelling with BVP

The MATLAB-code used for modelling Nernst-Plank equation as a boundary-value problem is presented below.

D.1 BVP script file

```
% MATLAB code for Master's Thesis in
% "Modelling of Membrane in a Sodium Sulfate Electrochemical Splitting
% Cell"
% written by Adna H. Carlberg
clc
clf
clear all
close all
global j MNa MH MO2 S L DNa DH DOH cS z F R T e v cNa_an cNa_cat cH_an
cH_cat cOH_an cOH_cat cH2O_an cH2O_cat U_an U_cat

%% Input parameters
cNa2SO4=1.921;       % Conc of sodium sulfate [M]
cNaOH=2.74;          % Conc of sodium hydroxide [M]
cH2SO4=1.853;        % Conc of sulfuric acid [M]
pH_an=-0.11;         % pH in anolyte at 80oC
pH_cat=11.43;        % pH in catholyte at 80oC
rho_an=1265.3;       % Density of anolyte [g/dm3]
rho_cat=1076.4;      % Density of anolyte [g/dm3]
my=0.5e-3;           % Dynamic viscosity [Pa*s](approx from AkzoNobel's
database)

i=3500;              % Current density [A/m2]
U_cell=4.2;          % Cell voltage/potential [V]
U_drop=0.1*U_cell;   % Potential drop 10% over membrane[V](Bulletin 95-
01)
U_an=2.1;      % GUESS! Potential at the anode side of the membrane [V]
U_cat=U_an-U_drop;   % Potential at the cathode side of the membrane[V]
T=80+273.15;         % Temperature [K]
P_an=0.56;           % Pressure in the anolyte [bar]
P_cat=0.7;           % Pressure in the catholyte [bar]
z=1;                 % Valence/charge number (Na+ & H+:z=1, OH-:z=-1)

%% Membrane specifications
S=100e-4;            % Active surface area of membrane [m2]
L=152.4e-6;          % Thickness of membrane [m]
DNa=0.98e-10;        % Diffusion coeff for Na+ [m2/s](N117)[Rakib-1999]
DH=3.5e-10;          % Diffusion coeff for H+ [m2/s](N117)[Rakib-1999]
DOH=1.6e-11;         % Diffusion coeff for OH- [m2/s](N324)[Davis-2006]
DH2O=9e-10;          % Diff. coeff for H2O [m2/s](N115)[Motupally,fig2]
e_r=20;              % Relative permittivity (Nafion 117)[Paddison-
1998,Schmidt-2010]
cS=1.5818;           % Concentration of sulfonate groups [M]
k=7.13e-20;          % Permeability [m2](Nafion 115)[Duan-2012]
phi=0.25;            % Porosity [%](Nafion 117)[Verbrugge-1988]

%% Constants
F=96485;             % Faradays number [A*s/mol]
R=8.3144621;         % Ideal gas constant [J/(K*mol)]
e0=8.85419e-12;      % Vacuum permittivity [F/m] or [A2*s4/(kg*m3)]
```

```
MNa2SO4=142.0376;    % Molar mass of sodium sulfate [g/mol]
MH2SO4=98.07354;     % Molar mass of sulfuric acid [g/mol]
MNaOH=39.99737;      % Molar mass of sodium hydroxide [g/mol]
MNa=22.99;           % Molar mass of sodium ion [g/mol]
MH=1.00797;          % Molar mass of hydrogen ion [g/mol]
MHSO4=97.06557;      % Molar mass of hydrogen sulfate [g/mol]
MSO4=96.0576;        % Molar mass of sulfate ion [g/mol]
MOH=17.00737;        % Molar mass of hydroxyl ion [g/mol]
MH2=2*1.00797;       % Molar mass of hydrogen [g/mol]
MO2=2*15.9994;       % Molar mass of oxygen [g/mol]
MH2O=18.01534;       % Molar mass of water [g/mol]

%% Calculated values
cNa_an=2*cNa2SO4;    % Conc of Na+ in the anolyte [M]
cNa_cat=cNaOH;       % Conc of Na+ in the catholyte [M]
cOH_an=0;            % GUESS! Conc of OH- in the catholyte [M]
cOH_cat=cNaOH;       % Conc of OH- in the catholyte [M]

conversion=cH2SO4/(cH2SO4+cNa2SO4); % Use eq.6 from [Fontes-1997]
cH_an=0.41*(cH2SO4+cNa2SO4);% Conc of H+ in the anolyte [M][Fontes-1997]
% cH_an=10^-pH_an;  % Conc of H+ in the anolyte, calc from pH
cH_cat=10^-pH_cat;  % Conc of H+ in the catholyte, calc from pH

cH2O_an=(0.6491*rho_an)/MH2O;
cH2O_cat=(0.9*rho_cat)/MH2O;

e=e_r*e0;                    % Absolute permittivity of Nafion [F/M]
q=-(k*(P_cat-P_an))/(my*L); % Flow through membrane [m3/(m2*s)]
v=q/phi;                     % Velocity through the membrane [m/s]

%% Solving BVP with Laplace
disp('BVP-Laplace')
% solinit=bvpinit(linspace(0,L,100),[cNa_an 0 cH_an 0 cOH_an 0 cH2O_an
0 U_an 0]);
solinit=bvpinit(linspace(0,L,3000),[cNa_an  ((cNa_cat-cNa_an)/L)  cH_an
((cH_cat-cH_an)/L)    cOH_an    ((cOH_cat-cOH_an)/L)    U_an    cH2O_an
((cH2O_cat-cH2O_an)/L) ((U_cat-U_an)/L)]);
% same solution when guessing slope for the profile, i.e. derivative
options=bvpset('Stats','on','RelTol', 1e-9,'AbsTol',[1e-12 1e-12 1e-12
1e-12 1e-12 1e-12 1e-12 1e-12 1e-12 1e-12 1e-12]);
sol=bvp4c(@odefunL,@odebc,solinit,options);
xint=linspace(0,L);
Sxint=deval(sol,xint);

figure(1)
plot(xint,Sxint(1,:),'g') % plots conc Na+ vs x
xlabel('Distance [m]')
ylabel('Concentration Na^+ [M]')
figure(2)
plot(xint,Sxint(3,:),'r') % plots conc H+ vs x
xlabel('Distance [m]')
ylabel('Concentration H^+ [M]')
figure(3)
plot(xint,Sxint(5,:),'k') % plots conc OH- vs x
xlabel('Distance [m]')
ylabel('Concentration OH^- [M]')
```

```
figure(4)
plot(xint,Sxint(7,:),'b') % plots potential vs x
xlabel('Distance [m]')
ylabel('Electric potential [V]')
figure(5)
plot(xint,-log10(Sxint(3,:)),'r') % plots pH vs x
xlabel('Distance [m]')
ylabel('pH profile')
figure(6)
plot(xint,Sxint(9,:),'b') % plots conc H2O vs x
xlabel('Distance [m]')
ylabel('Concentration H_2O [M]')
.
%% Calculating and plotting fluxes
Ni_Na=-DNa.*Sxint(2,:)-((z.*F.*DNa.*Sxint(1,:).*Sxint(8,:))./(R.*T));
Ni_H=-(DH.*Sxint(4,:))-((z.*F.*DH.*Sxint(3,:).*Sxint(8,:))./(R.*T));
Ni_OH=-DOH.*Sxint(6,:)-((-z.*F.*DOH.*Sxint(5,:).*Sxint(8,:))./(R.*T));
Ni_H2O=4.*Ni_Na+3.*Ni_H;

figure(7)
plot(xint,Ni_Na,'g')
xlabel('Distance [m]')
ylabel('Flux of Na^+ [mol/m^2s]')
figure(8)
plot(xint,Ni_H,'r')
xlabel('Distance [m]')
ylabel('Flux of H^+ [mol/m^2s]')
figure(9)
plot(xint,Ni_OH,'k')
xlabel('Distance [m]')
ylabel('Flux of OH^- [mol/m^2s]')
figure(10)
plot(xint,Ni_H2O,'b')
xlabel('Distance [m]')
ylabel('Flux of H_2O [mol/m^2s]')
```

D.2 Function files

```
function [dydx]=odefunL(x,y)
% System of 10 first-order ODEs
global z F R T
dydx(1)=y(2);                                          % conc Na+
dydx(2)=-((z*F)/(R*T)).*y(8).*y(2);
dydx(3)=y(4);                                          % conc H+
dydx(4)=-((z*F)/(R*T)).*y(8).*y(4);
dydx(5)=y(6);                                          % conc OH-
dydx(6)=-((-z*F)/(R*T)).*y(8).*y(6);
dydx(7)=y(8);                                          % Potential
dydx(8)=0;                                             % Laplace
dydx(9)=y(10);                                         % conc H2O
dydx(10)=(-4.*(dydx(2)+((z*F)/(R*T)).*y(8).*y(2))-
3.*(dydx(4)+((z*F)/(R*T)).*y(8).*y(4)));
dydx=dydx';
end
```

```
function [res]=odebc(ya,yb)
% Boundary conditions for 10 first-order ODEs
global cNa_an cNa_cat cH_an cH_cat cOH_an cOH_cat cH2O_an cH2O_cat
U_an U_cat
res(1)=ya(1)-cNa_an;
res(2)=yb(1)-cNa_cat;
res(3)=ya(3)-cH_an;
res(4)=yb(3)-cH_cat;
res(5)=ya(5)-cOH_an;
res(6)=yb(5)-cOH_cat;
res(7)=ya(7)-U_an;
res(8)=yb(7)-U_cat;
res(9)=ya(9)-cH2O_an;
res(10)=yb(9)-cH2O_cat;
res=res';
end
```

E MATLAB-code for Modelling with PDE

The MATLAB-code used for modelling Nernst-Plank as partial differential equations is presented below.

E.1 PDE script file

```
% MATLAB code for Master's Thesis in
% "Modelling of Membrane in a Sodium Sulfate Electrochemical Splitting
Cell"
% written by Adna H. Carlberg
clc
clf
clear all
close all
global F L L2 DNa1 DH1 DOH1 DNa2 DH2 DOH2 DH2O z R T e1 e_a e_c cNa_an
cNa_cat cH_an cH_cat cOH_an cOH_cat L1 DNa_a DH_a DOH_a L3 DNa_c DH_c
DOH_c U_an U_cat U_a U_c

%% Input parameters
cNa2SO4=1.921;      % Conc of sodium sulfate [M]
cNaOH=2.74;         % Conc of sodium hydroxide [M]
cH2SO4=1.853;       % Conc of sulfuric acid [M]
pH_an=-0.11;        % pH in anolyte at 80oC
pH_cat=11.43;       % pH in catholyte at 80oC
rho_an=1265.3;      % Density of anolyte [g/dm3]
rho_cat=1076.4;     % Density of anolyte [g/dm3]
my=0.5e-3;          % Dynamic viscosity [Pa*s](approx from AkzoNobel's
database)

i=3500;             % Current density [A/m2]
U_cell=4.2;         % Cell voltage/potential [V]
U_drop=0.1*U_cell;  % Potential drop 10% over membrane [V] (Bulletin
95-01)
U_an=2.1;           % GUESS! Potential at the anode side of the
membrane [V]
U_cat=U_an-U_drop;  % Potential at the cathode side of the membrane [V]
T=80+273.15;        % Temperature [K]
e_w=87.836914-0.396351*T+0.000745*T*T;   % Permittivity for water
[Verbrugge-1992]
P_an=0.56;          % Pressure in the anolyte [bar]
P_cat=0.7;          % Pressure in the catholyte [bar]
z=1;                % Valence/charge number (Na+ & H+:z=1, OH-:z=-1)

%% Membrane specifications
S=100e-4;           % Active surface area of membrane [m2]
L=152.4e-6;         % Thickness of membrane in total [m]
L2=127e-6;          % Thickness of membrane layer towards the anolyte
[m]
DNa1=0.98e-10;       % Diffusion coeff for sodium ion [m2/s](Nafion
117)[Rakib-1999]
DH1=3.5e-10;         % Diffusion coeff for hydrogen ion [m2/s](Nafion
117)[Rakib-1999]
DOH1=1.6e-11;        % Diffusion coeff for hydroxyl ion [m2/s](Nafion
324)[Davis-2006]
DH2O1=9e-10;         % Diffusion coeff for water [m2/s](Nafion
115)[Motupally, fig 2]
```

```
e_r=20;              % Relative permittivity (Nafion 117)[Paddison-
1998,Schmidt-2010]
cS=1.5818;          % Conc of sulfonate groups [M]
k=7.13e-20;         % Permeability [m2](Nafion 115)[Duan-2012]
phi=0.25;           % Porosity [%](Nafion 117)[Verbrugge-1988]

%% Boundary layer on anolyte side
L1=10e-6;               % GUESS! Film thickness [m]
K_an=30.3;              % Conductivity of the anolyte [S/m]
(AkzoNobel's database)
U_drop_an=(i/K_an)*L1;  % Potential drop over the anolyte boundary
layer [V]
U_a=U_an+U_drop_an;     % Potential at the anolyte side of the film [V]
DNa_a=1.11e-9;          % Diffusivity of sodium ion [m2/s][Bosander-1999]
DH_a=3.33e-9;           % GUESS! 3 times higher than DNa_a [m2/s]
DOH_a=4.43e-9;          % Diffusivity of hydroxyl ion [m2/s][Bosander-
1999]

%% Boundary layer on catholyte side
L3=10e-6;               % GUESS! Film thickness [m]
K_cat=69;               % Conductivity of the anolyte [S/m]
(AkzoNobel's database)
U_drop_cat=(i/K_cat)*L3; % Potential drop over the catholyte boundary
layer [V]
U_c=U_cat-U_drop_cat;   % Potential at the catholyte side of the film
[V]
DNa_c=1.11e-9;          % Diffusivity of sodium ion [m2/s][Bosander-1999]
DH_c=3.33e-9;           % GUESS! 3 times higher than DNa_c [m2/s]
DOH_c=4.43e-9;          % Diffusivity of hydroxyl ion [m2/s][Bosander-
1999]

%% Constants
F=96485;            % Faradays number [A*s/mol]
R=8.3144621;        % Ideal gas constant [J/(K*mol)]
e0=8.85419e-12;     % Vacuum permittivity [F/m] or [A2*s4/(kg*m3)]

MNa2SO4=142.0376;   % Molar mass of sodium sulfate [g/mol]
MH2SO4=98.07354;    % Molar mass of sulfuric acid [g/mol]
MNaOH=39.99737;     % Molar mass of sodium hydroxide [g/mol]
MNa=22.99;          % Molar mass of sodium ion [g/mol]
MH=1.00797;         % Molar mass of hydrogen ion [g/mol]
MHSO4=97.06557;     % Molar mass of hydrogen sulfate [g/mol]
MSO4=96.0576;       % Molar mass of sulfate ion [g/mol]
MOH=17.00737;       % Molar mass of hydroxyl ion [g/mol]
MH2=2*1.00797;      % Molar mass of hydrogen [g/mol]
MO2=2*15.9994;      % Molar mass of oxygen [g/mol]
MH2O=18.01534;      % Molar mass of water [g/mol]

%% Calculated values
cNa_an=2*cNa2SO4;   % Conc of Na+ in the anolyte [M]
cNa_cat=cNaOH;      % Conc of Na+ in the catholyte [M]
cOH_an=0;           % GUESS! Conc of OH- in the catholyte [M]
cOH_cat=cNaOH;      % Conc of OH- in the catholyte [M]

conversion=cH2SO4/(cH2SO4+cNa2SO4); % Use eq.6 from [Fontes-1997]
cH_an=0.41*(cH2SO4+cNa2SO4); % Conc of H+ in the anolyte [M][Fontes-1997]
% cH_an=10^-pH_an;  % Conc of H+ in the anolyte, calc from pH
cH_cat=10^-pH_cat;  % Conc of H+ in the catholyte, calc from pH
```

```
cH2O_an=(0.6491*rho_an)/MH2O;
cH2O_cat=(0.9*rho_cat)/MH2O;

e1=e_r*e0;                  % Absolute permittivity of Nafion [F/M]
e_a=e_w*0.65*e0;            % Absolute permittivity of boundary layer
on anolyte side [F/M]
e_c=e_w*0.9*e0;             % Absolute permittivity of boundary layer
on catholyte side [F/M]
q=-(k*(P_cat-P_an))/(my*L); % Flow through membrane [m3/(m2*s)]
v=q/phi;                    % Velocity through the membrane [m/s]

%% Numerical solution (Membrane+2 boundary layers)
tic
xmesh=linspace(0,(L1+L+L3),200);
tspan=linspace(0,1000,1e4);
m=0;
sol=pdepe(m,@pdefunL2,@pdeic2,@pdebc2,xmesh,tspan);
u1=sol(:,:,1);      % Na+
u2=sol(:,:,2);      % H+
u3=sol(:,:,3);      % OH-
u4=sol(:,:,4);      % potential
toc

%% Plots
figure(1) % create new figure
surf(xmesh,tspan,u1)            % 3D-plot with axis x,y,z
xlabel('Distance [m]')
ylabel('Time [s]')
zlabel('Conc [M]')
figure(2)
plot(xmesh,u1(end,:),'g')    % plots the conc profile at the last time
xlabel('Distance [m]')
ylabel('Concentration Na^+ [M]')
line([L1 L1],[2.6 4]);
line([L1+L L1+L],[2.6 4]);

figure(3)
surf(xmesh,tspan,u2)            % 3D-plot with axis x,y,z
xlabel('Distance [m]')
ylabel('Time [s]')
zlabel('Conc [M]')
figure(4)
plot(xmesh,u2(end,:),'r')    % plots the conc profile at the last time
xlabel('Distance [m]')
ylabel('Concentration H^+ [M]')
line([L1 L1],[0 1.8]);
line([L1+L L1+L],[0 1.8]);

figure(5)
plot(xmesh,-log10(u2(end,:)),'r') % plots y vs x
xlabel('Distance [m]')
ylabel('pH profile')
line([L1 L1],[-2 12]);
line([L1+L L1+L],[-2 12]);
```

```
figure(6)
surf(xmesh,tspan,u3)              % 3D-plot with axis x,y,z
xlabel('Distance [m]')
ylabel('Time [s]')
zlabel('Conc [M]')
figure(7)
plot(xmesh,u3(end,:),'k')     % plots the conc profile at the last time
xlabel('Distance [m]')
ylabel('Concentration OH^- [M]')
line([L1 L1],[0 3]);
line([L1+L L1+L],[0 3]);

figure(8)
surf(xmesh,tspan,u4)              % 3D-plot with axis x,y,z
xlabel('Distance [m]')
ylabel('Time [s]')
zlabel('Conc [M]')
figure(9)
plot(xmesh,u4(end,:))    % plots the potential profile at the last time
xlabel('Distance [m]')
ylabel('Electric potential [V]')
line([L1 L1],[1.6 2.1]);
line([L1+L L1+L],[1.6 2.1]);
```

E.2 Function files

```
function [a,f,s]=pdefunL2(x,t,u,dudx)
% Coefficients for rewritten PDEs
global F L L2 DNa1 DH1 DOH1 DNa2 DH2 DOH2 z R T e1 e_a e_c L1 DNa_a
DH_a DOH_a DNa_c DH_c DOH_c

% If one membrane layer
if x<=L1
    DNa=DNa_a;
    DH=DH_a;
    DOH=DOH_a;
    e=e_a;
elseif x>(L1+L)
    DNa=DNa_c;
    DH=DH_c;
    DOH=DOH_c;
    e=e_c;
else
    DNa=DNa1;
    DH=DH1;
    DOH=DOH1;
    e=e1;
end

% If two membrane layers
% if x<=L1
%     DNa=DNa_a;
%     DH=DH_a;
%     DOH=DOH_a;
% elseif  x>L1 && x<=(L1+L2)
%     DNa=DNa1;
%     DH=DH1;
```

```
%     DOH=DOH1;
% elseif x>(L1+L)
%     DNa=DNa_c;
%     DH=DH_c;
%     DOH=DOH_c;
% else
%     DNa=DNa2;
%     DH=DH2;
%     DOH=DOH2;
% end

a=[1;1;1;0];    % one column [Na,H,OH,potential]
f=[((dudx(1).*DNa)+((z.*F.*DNa.*u(1).*dudx(4))./(R.*T)));
    ((dudx(2).*DH)+((z.*F.*DH.*u(2).*dudx(4))./(R.*T)));
    ((dudx(3).*DOH)+((-z.*F.*DOH.*u(3).*dudx(4))./(R.*T)));
    -e.*dudx(4)];
s=[0;0;0;0];
end


function [u0]=pdeic2(x)
% Initial condition for PDEs
global L1 L

if x<=L1
    u0=[4.256;0;0;0];
elseif x>(L1+L)
    u0=[0.2;0;0.2;0];
elseif x>L1 && x<=(L1+L)
    u0=[0;0;0;0];
end
end


function [pl,ql,pr,qr]=pdebc2(xl,ul,xr,ur,t)
% Boundary conditions for PDEs
global cNa_an cNa_cat cH_an cH_cat cOH_an cOH_cat U_an U_cat U_a U_c

pl=[ul(1)-cNa_an; ul(2)-cH_an; ul(3)-cOH_an; ul(4)-U_a];
ql=[0;0;0;0];       % derivative
pr=[ur(1)-cNa_cat; ur(2)-cH_cat; ur(3)-cOH_cat; ur(4)-U_c];
qr=[0;0;0;0];
end
```

F Surface Plots for Concentration Profiles

The surface plots for the concentration profiles for the ions in time and space, from the PDE solution, is presented in this section. The end time for the time interval in the *pdepe*-solver is chosen so that the profiles are no longer changing shape. Important to point out is that the intervals are made coarser here in these plots to be able to distinguish the colors and change of shape of the concentration profile the beginning of time interval.

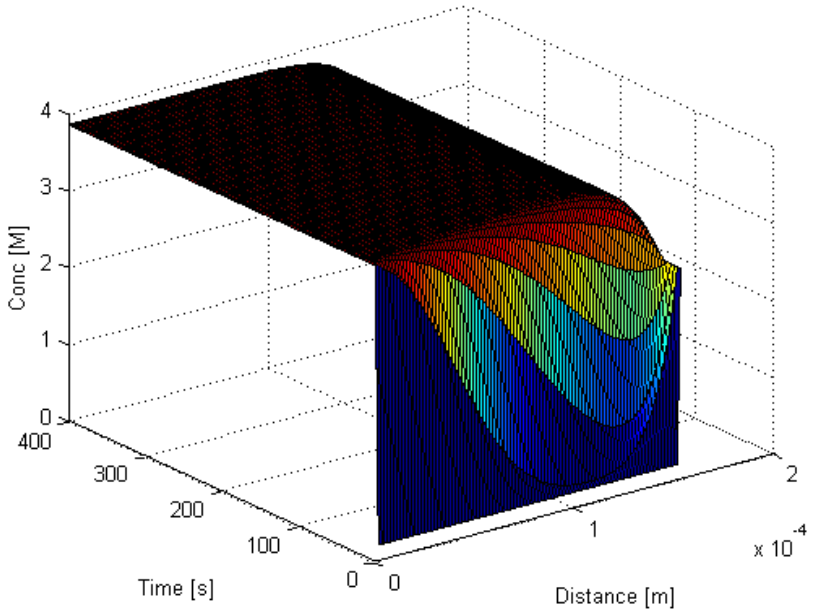

Figure 19: Concentration profile in time and space for sodium ions from PDE solution.

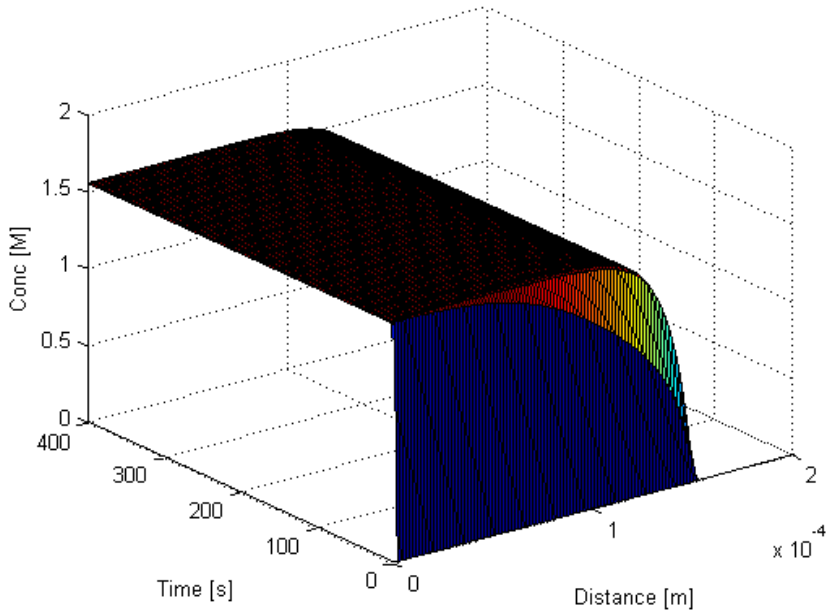

Figure 20: Concentration profile in time and space for hydrogen ions from PDE solution.

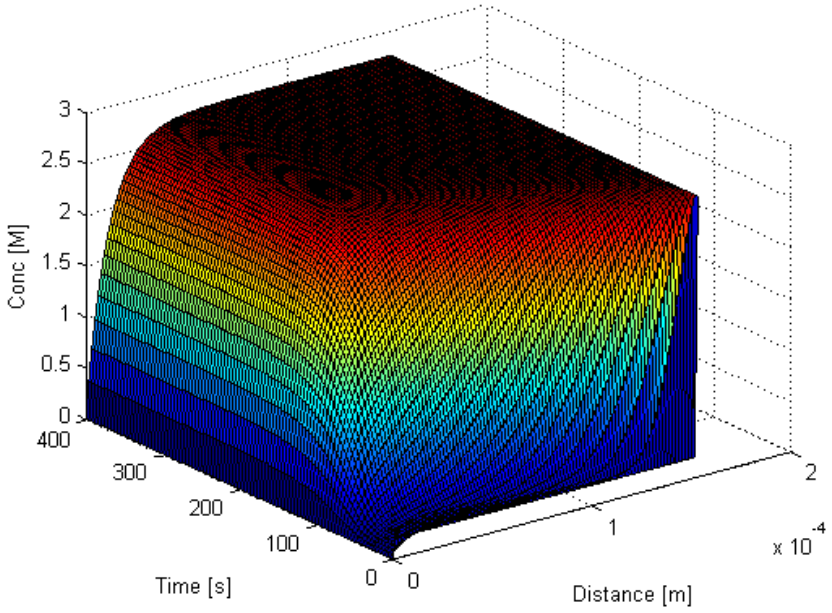

Figure 21: Concentration profile in time and space for hydroxyl ions from PDE solution.